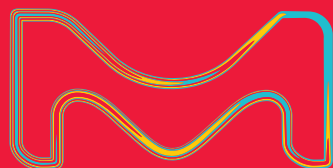


**Sigma-Aldrich**<sup>®</sup>

Lab Materials & Supplies



# Nanomaterial Bioconjugation Techniques

The future of bioimaging

Foreword by Dr. Greg Hermanson

The life science business of Merck operates as  
MilliporeSigma in the U.S. and Canada.

**MERCK**

# Nanotechnology Foreword



**Greg T. Hermanson**

Bioscience Consultant and Author of *Bioconjugate Techniques*

Although the revolution in nanotechnology had its start less than twenty-five years ago, it has quickly become one of the strongest growth areas within science and technology. The use of new nanomaterials combined with novel applications has fueled an engine of innovation that has impacted many areas of research and development. It has made possible new sensitive assay and detection platforms, diagnostic assays, *in vivo* imaging capabilities, therapeutic treatments, and even several exciting consumer products.

However, the application of nanotechnology in materials and products is not entirely new; in fact, it actually extends far into the past. Nanomaterials have been used for centuries, despite the fact that their composition and properties were not clearly understood until relatively recently. Perhaps the first characterized construction of nanoparticles dates back to Michael Faraday's preparation of a ruby red suspension of colloidal gold in 1857. Over a century later, this same type of colloidal suspension has found important application as a detection reagent in immunoassays. Once conjugated with antibodies, these ancient particles have the potential to form a highly-specific disease diagnostic platform, with intense signal and localized antigen specificity.

It may have been Richard Feynman, however, a leading theoretical physicist, who had the first vision of how nanomaterials could transform material science and its applications. In a lecture Feynman gave in 1959 at the California Institute of Technology entitled "There's Plenty of Room at the Bottom", he envisioned precisely engineered nano-structures made and manipulated with highly configurable properties. This vision would eventually revolutionize many technological fields. Feynman noted, "It is a staggeringly small world that is below. In the year 2000, when they look back at this age, they will wonder why it was not until the year 1960 that anybody began seriously to move in this direction."

Yet it wasn't until the early 1990s that a number of methods describing the design of a variety of new and fascinating nanoscale structures began to appear in scientific literature. These nanoparticle constructs quickly started impacting a number of important fields in the life sciences, medicine, electronics, and the material sciences. Many of the most interesting of these small structures were less than 100 nm in

diameter and some even approached the small size of biological macromolecules. At this same time, the term nanotechnology was first coined, and by its official designation, helped create an exciting new field that combined the novel nanoscale characteristics of materials with their unique applications in a variety of high technology areas.

By the year 2000, nanotechnology was a widely discussed topic and government initiatives were initiated in order to create a long-term vision with a funding mechanism for research into virtually anything involving nano. Numerous scientific journals and magazines were quickly founded and eventually billions of dollars flowed into nanotechnology programs worldwide. Today, the world of nanotechnology has blossomed into a mature field with a broad selection of nanomaterials for applications as diverse as electronic circuitry, incredibly bright and colorful displays, extremely sensitive biosensors, as novel detection reagents using various light-based techniques, and even as therapeutic agents to fight disease.

For many of these applications, the ability to conjugate another molecule to the surface of a nanomaterial is a critical factor to their successful use. Especially for biological applications, the conjugation process often involves the covalent coupling of an antibody or another affinity ligand to a nanoparticle to create a nano-bioconjugate. The affinity molecule thus provides the capture or targeting capabilities of the complex (e.g., to a specific antigen) while the nanomaterial contributes signal generation and detection capabilities.

This guide reviews how nanomaterial conjugates can be used in life science applications and clinical diagnostics. Currently, most of the available diagnostics tools rely on magnetic, fluorescence or optical based detection and accordingly the guide is segmented into three sections. Each segment of the guide contains a micro-review article on the diagnostics techniques and methods elaborating on the bioconjugation of respective nanomaterials. Thus, the guide describes the most important new materials in nanotechnology available today in practical terms, allowing both experts and novices to quickly combine the power of bio plus nano in virtually any configuration imaginable.

# Introduction



## Niraj Singh

Product Manager - Energy Materials  
MilliporeSigma, Milwaukee, WI USA  
Email: niraj.singh@sial.com

## Bryce Nelson

Head of Materials Science  
MilliporeSigma, Milwaukee, WI USA  
Email: bryce.nelson@sial.com

The concept of nanotechnology was defined in 1959, but the benefits of nanoscience have taken decades to realize. Progress in biomedical applications of nanotechnology have been particularly slow, in large part due to the need for effective conjugation chemistry for the attachment of biomolecules such as peptides, oligonucleotides, antibodies, or proteins to the nanomaterial surface.<sup>1-6</sup>

Despite this slow progress, the use of nanomaterials in diagnostics has enormous potential and has recently accelerated.<sup>1-4</sup> Because nanomaterials are the same size as proteins and other cellular components ( $\leq 100$  nm), they can interact with living cells and their constituents in unique ways.<sup>5</sup> Thus, biomolecule-nanomaterial conjugates have the potential for many applications, including early and rapid disease detection. This guide is intended to provide detailed protocols for the conjugation of the major classes of nanomaterials used in both current and future diagnostics applications (**Figure 1**).

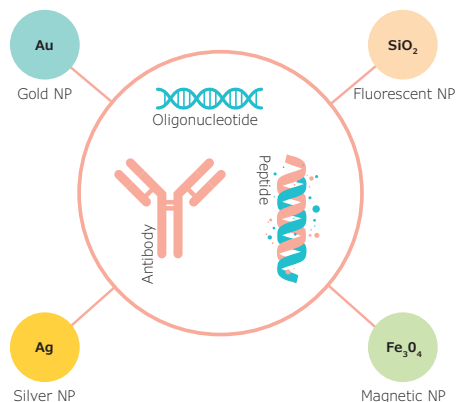


**Figure 1.** Schematic summarizing the major components of a biomolecule-nanomaterial conjugate used in the development and application of a diagnostic assay.

In this guide, we discuss the chemistry required for successful conjugation of nanomaterials used in the development of current and future diagnostics such as immunoassays, flow cytometry, cellular imaging, and genomic analysis. We have segmented this guide according to the three most commonly employed detection methods (magnetic, fluorescent, and optical detection) and highlighted conjugation methods for use with the associated nanoparticles used to generate the

*Continued next page.*

# Table of Contents

## Articles

### Magnetic Imaging

Biomedical Applications of Magnetic Micro- and Nanoparticles **3**

Jon Dobson

Method: Conjugation Protocols for Magnetic Nanoparticles **8**

Xin Ji, Y. Andrew Wang

### Fluorescence-based Imaging

Fluorescent Nanoparticles for Imaging and Diagnostics **14**

Maria Ada Malvindi, Enrico Binetti, Pier Paolo Pomba

Method: Fluorescent Silica Nanoparticle Bioconjugation **17**

Maria Ada Malvindi, Enrico Binetti, Pier Paolo Pomba

### Optical Imaging

Plasmonic Materials and Their Applications in Diagnostics **22**

Bo Zhang, Jeyarama S. Ananta, Meijie Tang, Hongjie Dai

Method: Conjugation of Proteins to Gold Nanoparticles **26**

Benny Pacheco

Method: Conjugating Gold Nanorods to Streptavidin and IgG **31**

Christian Schoen

Method: Directional Antibody Conjugation of Silica-coated Gold Nanoparticles **33**

Justin Harris, Brantley Henson, Jason Cook, Kimberly Homan

Method: Covalent Bioconjugation of Antibodies to Carboxyl Terminated Nanoparticles **37**

Rhea Decker, Steven J. Oldenburg

## Featured Products

Iron Oxide Nanoparticles **12**

Fluorescent Silica Nanoparticles **20**

Silica Nanospheres **20**

Monodispersed Nanodiamonds **20**

Gold Nanoparticles and Nanostructures **40**

Non-surface Functionalized Nanoparticles and Nanostructures **40**

Surface-functionalized Nanoparticles and Nanostructures **41**

Silver Nanoparticles and Nanostructures **43**

detection signal. For example, many iron oxide nanoparticles possess superparamagnetic properties that enable magnetic resonance based imaging with resolution at the micron level.<sup>7-8</sup> Silica nanoparticles with encapsulated fluorophores generate a fluorescent signal with remarkable photostability and brightness and have been shown to achieve resolution at the molecular level.<sup>9-10</sup> Gold and silver nanoparticles generate strong optical signals arising from surface plasmons and have been successfully implemented in diagnostic applications. Many of these applications are based on surface enhanced Raman or fluorescence techniques that achieve unprecedented sensitivity. However, it must be emphasized that effective conjugation chemistry is essential for the success of any assay involving nano-sized materials.

The first section discusses magnetic detection methods enabled by magnetic nanomaterials. Here, Prof. Jon Dobson (University of Florida, USA) reviews biomedical applications of iron oxide nanoparticles in cell separation, magnetic resonance imaging (MRI), drug delivery, magnetic hyperthermia, and gene transfection. Different strategies and methods for bioconjugation of iron oxide nanoparticles with varying surface functional groups with antibodies, proteins, and enzymes are also discussed here. The section also summarizes some of the common techniques used in characterizing iron-oxide nanoparticle-bioconjugates.

The second section focuses on fluorescent detection methods. Dr. Pier Paolo Pompa (Istituto Italiano di Tecnologia, Italy) begins this section by elaborating on the use of fluorescent

nanoparticles in diagnostics development. Special attention is paid to the use of fluorescent silica nanoparticles. Bioconjugation protocols of silica nanoparticles with DNA and antibodies are also presented in this section.

The third section of this guide focuses on techniques that utilize the unique optical properties of metallic nanoparticles. In this section, Prof. Hongjie Dai (Stanford University, USA) reviews the plasmonic properties of metallic nanoparticles and their potential use in diagnostics. Protocols that illustrate the bioconjugation of newly developed nanoparticles and nanostructures such as nanorods, nanourchins, and nanoplates are also presented in this section.

## References

- (1) Biju, V. *Chem. Soc. Rev.* **2014**, *43*, 744.
- (2) Strong, L. E.; West, J. L. *ACS Biomater. Sci. Eng.* **2015**, *1*, 685
- (3) Giner-Casares, J. J.; Henriksen-Lacey, M.; Coronado-Puchau, M.; Liz-Marzan, L. M. *Mater. Today*. **2016** *19*, 19.
- (4) Howes, P. D.; Rana, S.; Stevens, M. M.; *Chem. Soc. Rev.* **2014**, *43*, 3835.
- (5) Tram, D. T. N.; Wang, H.; Sugiarto, S.; Li, T.; Ang, W. H.; Lee, C.; Pastorin, G. *Biotechnol. Adv.* **2016**, *34*, 1275.
- (6) Oliveira Jr., O. N.; Iost, R. M.; Siqueira Jr., J. R.; Crespihlo, F. N.; Caseli, L. *ACS Appl. Mater. Interfaces*. **2014**, *6*(17), 14745-14766.
- (7) Heng, L.; Zhang, J.; Chen, X.; Du, X.-S.; Zhang, J.-L.; Gang, L.; Zhang, W.-G.; *Nanoscale*, **2016**, *8*, 7808-7826.
- (8) Li, L.; Jiang, W.; Luo, K.; Song, H.; Lan, F.; Wu, Y.; Gu, Z.; *Theranostics*, **2013**, *3*, 595-615.
- (9) Burns, A.; Ow, H.; Wiesner, U.; *Chem. Soc. Rev.*, **2006**, *35*, 1028-1042.
- (10) Peuschel, H.; Ruckelshausen, T.; Cavelius, C.; Kraegeloh, A.; *BioMed Research International*, **2015**, *2015*, 961208.

**Sigma-Aldrich**<sup>®</sup>  
Lab Materials & Supplies

# IMPROVE DELIVERY

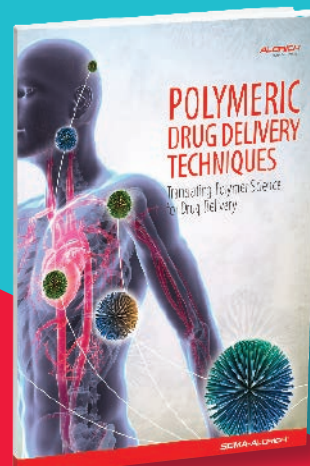
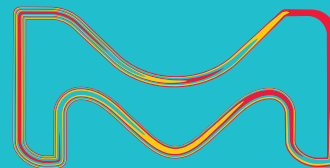
## A Step-by-Step Guide

Low drug solubility and stability often reduce the effectiveness of an otherwise promising therapeutic candidate. In this comprehensive guide, you'll discover how polymers can provide the drug delivery solutions you need for controlled release, targeting, and solubility enhancement.

Request your copy online at:

**[SigmaAldrich.com/ddtechnique](http://SigmaAldrich.com/ddtechnique)**

The life science business of Merck operates as MilliporeSigma in the U.S. and Canada.



**MERCK**

# Biomedical Applications of Magnetic Micro- and Nanoparticles



Jon Dobson

J Crayton Pruitt Family Department of Biomedical Engineering and Department of Materials Science and Engineering, University of Florida Gainesville, Florida 32611, USA  
Email: jdobson@bme.ufl.edu

## Introduction

Magnetic micro- and nanoparticles offer great promise for applications in biomedical research and clinical therapies. The use of magnetic particles in biological research applications dates to the 1920s when two researchers, William Seifriz and L.V. Heilbrunn, independently published papers describing experiments using Ni and Fe microparticles to probe the physical properties of cellular "protoplasm".<sup>1,2</sup> By measuring the change in time for particles moving through the viscous medium and calculating force on the particles within the field gradient, Seifriz and Heilbrunn were able to evaluate viscosity and elasticity of the protoplasm.

After more than 20 years, the idea of using the motion of magnetic particles in fields to investigate cellular properties was revived by an unlikely researcher, Francis Crick. Together with A.F.W. Hughes, they refined previous work by Seifriz and Heilbrunn and introduced the concept of "magnetic twisting" by utilizing the motion of magnetically blocked particles in rotating fields.<sup>3</sup> This twisting idea would later form the basis of magnetic twisting cytometry, in which magnetic particles are attached to integrin receptors on the cell surface, magnetized, and twisted in a rotating field. As the integrins are coupled to the internal cellular cytoskeleton, measuring the twisting force of the attached particles enables measurement of the mechanical properties of the cytoskeleton.<sup>4,5</sup>

Since their initial use *in vitro*, magnetic micro- and nanoparticles have been used in many new biomedical applications, both in the laboratory and the clinic. Magnetic nanoparticles (MNPs) couple very strongly to applied magnetic fields in comparison to "non-magnetic" (diamagnetic) materials. As the human body is diamagnetic and largely unaffected by magnetic fields, externally applied fields can be used to remotely manipulate MNPs within the body or to transfer energy from the field to the particles for applications.

The most significant clinical application of MNPs is likely the exploitation of their magnetic behavior in strong, static magnetic fields on proton motion in magnetic resonance imaging (MRI) to provide image contrast. In this overview, we will discuss a selection of biomedical applications for magnetic nanoparticles.

## MRI Contrast Enhancement

The principles of magnetic resonance (MR) image generation are similar to those of nuclear magnetic resonance (NMR). Within the body, hydrogen protons in water molecules align both parallel and antiparallel to the strong, static magnetic field of the MR magnet. A radiofrequency (RF) field is applied in the plane perpendicular to the field axis and as this field is matched to the natural (Larmor) precession frequency of the hydrogen protons in the water, they are knocked out of alignment with the field. Once the RF field is removed, the protons precess back into alignment with the static field. This return to alignment consists of two components that can be measured; (i) the growth of the signal along the field axis as the protons return to alignment with the field, and (ii) the decay of the signal in the plane perpendicular to the field axis as the proton spins lose phase coherence once the RF field is removed. These two signals are known as  $T_1$  and  $T_2$ , respectively.

Introducing magnetic iron oxide nanoparticles (often called superparamagnetic iron oxides or SPIONs) into the body enhances the static field in regions with particles (**Figure 1**).<sup>6</sup> This local enhancement of the static field by MNPs is due to the alignment of the magnetization vector of the particles with the field, which speeds up proton dephasing, and causes contrast in the  $T_2$  signal. While the generation of the actual image is a bit more complex, it is easy to see how MNPs can be used to enhance MRI contrast, particularly if they are functionalized or coated with biomolecules to target certain cell types. In addition, MNPs tend to accumulate in the liver and spleen, as well as in solid tumors, due to their "leaky vasculature," which can highlight these organs and structures in  $T_2$ -weighted MR images.

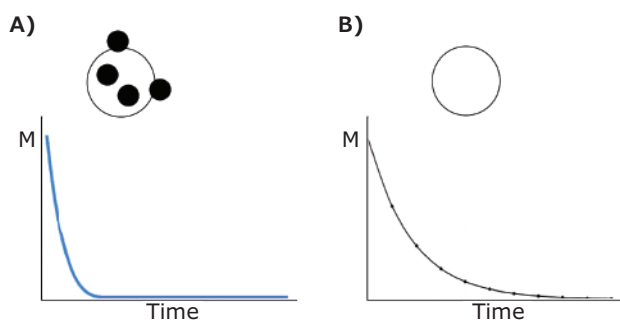


**Figure 1.** Effect of magnetic particle internalization in cells on  $T_2^*$  relaxation times: **A)** the protons in cells tagged by magnetic particles have a shorter  $T_2^*$  relaxation time than those in **B)** untagged cells.<sup>18</sup>

### Magnetic Separation of Cells and Biomolecules

Magnetic micro- and nanoparticles are also regularly used in biomedical laboratories. The force of attraction between the particles and magnetic fields with a high gradient enables the separation of specific target biomolecules and cells from biological liquid samples, such as blood and urine,<sup>7,8</sup> for both research and therapy. In this application, magnetic particles are functionalized with antibodies or biomolecules that bind to specific cell surface receptors or to biomolecules, such as target proteins. The biofunctionalized particles are mixed with the fluid containing the cells or biomolecules of interest, and then passed through a high-gradient magnetic separator (**Figure 2**). The magnetic separator may consist of a “soft” magnetic mesh that is magnetized in the presence of a field, or it may be composed of high-gradient magnets placed outside the separation tube. As the fluid/particle mixture passes through the separator, the magnetic particles are attracted to the field source holding them in place along with their targets, while the remaining (non-particle-tagged) fluid, cells, and proteins pass through. Once all of the fluid has passed through the separator, the field can be turned off, demagnetizing the mesh, or the magnet can be removed from the side of the separator. The removal of the attractive force allows the particles and the cells/biomolecules to which they are bound to be washed through and collected.

### Magnetic Drug Targeting

In the late 1970s, Widder and colleagues began to explore the use of magnetic particles and magnetic fields to focus the delivery of therapeutic drugs to specific sites in the body.<sup>9</sup> The researchers reasoned that if a drug, such as a chemotherapy compound, could be conjugated to a magnetic nanoparticle and injected into the vasculature, it could be used to target a specific site (e.g., a tumor) by focusing a strong, high-gradient field over the body at the location of the tumor. Despite being around for decades, this method is not routinely used in the clinic for several reasons. For example, external magnet sources cannot readily generate sufficient force on magnetic nanoparticles traveling through the vasculature. In addition, the use of an external magnet source traps the particle/drug complex in tissue closest to the body’s surface rather than in deeper tissue, potentially preventing the drug from entering tumors deep in the body (**Figure 3**).

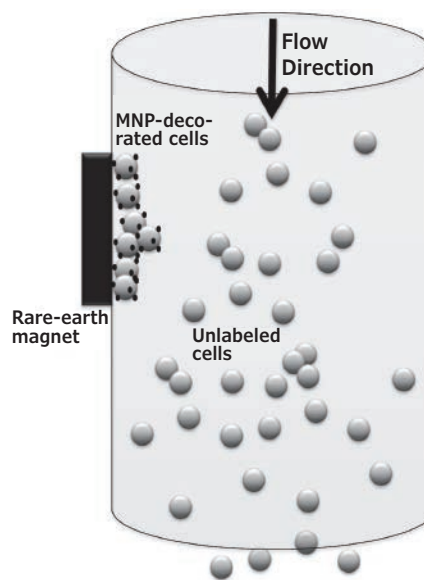


**Figure 2.** Principles of magnetic cell separation. Cells in suspension decorated with magnetic micro- or nanoparticles are attracted to the magnet as they pass through the column. Unlabeled cells pass through without being captured. After the sample has cleared the column, the magnet is removed, and the supernatant is washed out with the target cells. Note: MNP, magnetic nanoparticle.<sup>8</sup>

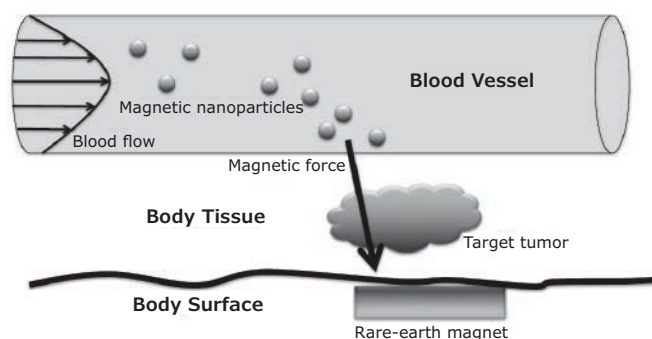


**Figure 3.** Principles of magnetic targeting for drug delivery. Magnetic nanoparticles carrying a therapeutic agent are pulled from circulation by a high gradient magnetic field positioned at the target site (such as a tumor). The magnetic nanoparticles collect at the target site and exit the vasculature via an enhanced permeability and retention effect.<sup>8</sup>

Methods to eliminate these issues are currently being explored, such as using Halbach arrays to generate higher gradient fields,<sup>10</sup> implanting magnetizable meshes near the target site,<sup>11</sup> using MRI magnets to “steer” MNP-therapeutic agent conjugation, and developing “magnetic pushing” technologies.<sup>12</sup> While interesting, a lack of solutions for these critical issues has prevented clinical translation of this concept.

## Nanomagnetic Gene Transfection

The promise of gene therapies and a better understanding of genetic diseases with the sequencing of the human genome remains unfulfilled to a large degree. One of the main issues with gene therapy and the use of genetically modified cells, tissues, and organisms to study these diseases, is the difficulty in delivering genes of interest into cells. While viruses are exceptionally efficient at gene delivery, they face significant limitations both in clinical use and genetic research.

In the clinic, safety issues are associated with using attenuated viruses to carry the genetic payload. These issues include insertional mutagenesis (inserting the gene in the wrong location within the chromosome, which can potentially activate oncogenes or turn off tumor suppressor genes), and limitations in plasmid size. These limitations have led to increased efforts to develop non-viral forms of gene transfection and delivery.

In 2000, our group demonstrated the first use of magnetic particles for targeted gene delivery *in vitro*. The green fluorescent protein (GFP) reporter gene was packaged within an adeno-associated virus (AAV) and conjugated to magnetic microspheres.<sup>13,14</sup> High-gradient, rare earth magnets were placed beneath a cell culture plate, guiding the particle-virus complex to a specific site within the dish, which resulted in the transfection of cells only at the magnet site (**Figure 4A–4D**).

At the same time, Plank and coworkers developed a similar technology that eliminated the need for viral carriers. Their method utilized the adsorption of negatively charged plasmid DNA onto magnetic iron oxide nanoparticles coated with positively charged polymers.<sup>15</sup> While the technique proved to be rapid and effective *in vitro*, transfection efficiency was not high in all cell types and *in vivo* translation has proven difficult. However, with the capacity to delivery large plasmids, such as those associated with diseases such as Parkinson's disease, rapid transfection, and high cell viability, "magnetofection" proved to have significant advantages for *in vitro*, non-viral transfection.

A few years later, our group developed arrays of oscillating magnets to improve magnetofection transfection efficiency (**Figure 4E–4F**).<sup>16</sup> The mechanical stimulation improved uptake and release from endosomal compartments in many cell types, resulting in higher transfection efficiency with no impact on cell viability. Current work in this area focuses on novel magnet array designs, as well as improvements to particle characteristics with the aim of increasing transfection efficiency and facilitating clinical translation.

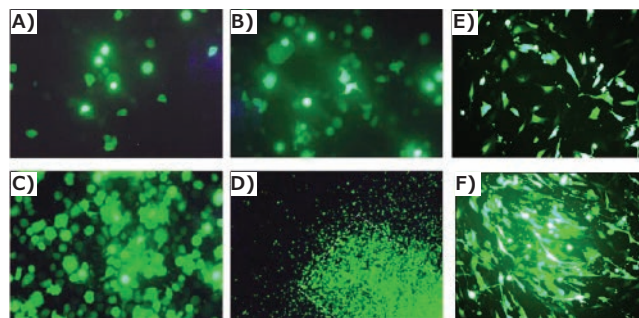


**Figure 4.** A–D) *in vitro* transduction of c12S cells via rAAV-GFP-magnetic microsphere conjugates. Panel D) shows the outline of the NdFeB magnet below the culture plate.<sup>14</sup> Static E) vs. oscillating F) magnetofection of GFP reporter constructs in NIH 3T3 cells.

## Magnetic Fluid Hyperthermia

The concept of using heat to destroy tumors and treat cancer goes back more than 4,000 years.<sup>17</sup> One of the key difficulties with this form of therapy is heating the tumor (to cause apoptosis or necrosis) without damaging healthy tissue surrounding the tumor. To address this issue, researchers have investigated the use of magnetic nanoparticles and radiofrequency magnetic fields in magnetic fluid hyperthermia (MFH). Since the initial experimental work by Gilchrist and colleagues in the 1950s, numerous studies on both the theoretical foundations as well as the development of optimized particles for MFH have been published.<sup>18,19</sup> The bulk of current research in magnetic fluid hyperthermia is focused in three broad areas: (i) optimizing particles and coatings to generate efficient energy/heat transfer (increased specific absorption rate—SAR),<sup>20</sup> (ii) understanding the mechanisms responsible for energy transfer and cellular responses on the nanoscale,<sup>21</sup> and (iii) development of efficient targeting and tumor loading strategies.

The central tenant of this technique is that iron oxide magnetic nanoparticles introduced into a solid tumor, either via direct injection or intravenous injection and passive (leaky tumor vasculature) or active (antibody) targeting, will couple more strongly to an applied RF magnetic field compared to the surrounding non-magnetic (diamagnetic) tissue. By coupling to the field, energy can be transferred from the field to the particles and dissipated in the form of heat. By raising the temperature of the cancer cells within the tumor to 40–42 °C, cancer cell death can be caused by either apoptosis, necrosis of the MNP-loaded tumor, or sensitization of the MNP-targeted cancer cells by increasing response to radio- or chemotherapy (adjuvant MFH).<sup>22</sup>

## Magnetic Actuation of Cell Surface Receptors

In recent years, new biomedical applications of magnetic nanoparticles have begun to emerge. Our group is currently developing technology for magnetically-activated receptor signaling (MARS). MARS relies on the fact that cell signaling is controlled by conformational changes to receptors on cell surfaces. These changes are normally driven by ligand binding, changes in cell membrane potential, or mechanical deformation/conditioning. The activation of cell surface receptors enables control of cell functions, such as apoptosis, migration, division,

and tissue matrix production. By functionalizing MNPs with molecules that target (but do not necessarily activate) these surface receptors, MNP-targeting molecule conjugates can be used as remote receptor actuators via the application of applied magnetic fields (**Figure 5**).<sup>23,24</sup> We are currently developing MARS for applications in stem cell therapy, drug discovery, tissue engineering, and regenerative medicine. Variations in this concept can also be used to control the activation of death receptors in cancer cells.<sup>25</sup>

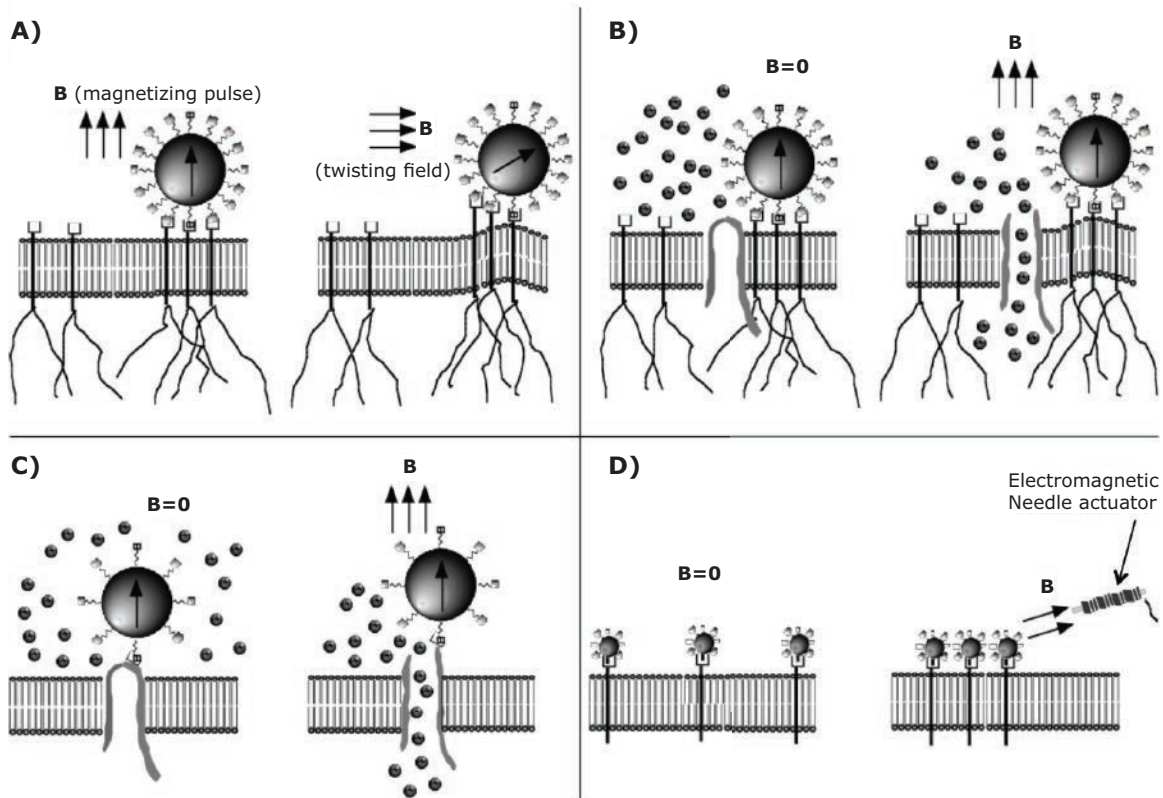


**Figure 5.** Schematic representation of different types of nanomagnetic actuation: **A)** Magnetic Twisting Cytometry: Large (micron-sized) magnetic particles are linked to actin filaments via integrin receptors bound to RGD molecules coated onto the particle surface. A magnetizing pulse is applied (left) which gives the particle a remanent magnetization ( $B$  = magnetic field vector). A torque is then applied (right) to the particle via a “twisting field” and the force required to twist the particle is related to the mechanical properties of the actin filaments. **B)** Mechanosensitive Ion Channel Activation: Magnetic particles are bound to the integrin receptors (left) and, upon the application of a high-gradient magnetic field (left) the particles are pulled towards the field, deforming the cell membrane and activating adjacent mechanosensitive ion channels. **C)** Magnetically Activated Receptor Signaling (MARS): Magnetic nanoparticles are attached to a cell surface receptor—in this example, an ion channel—via an antibody (left). Upon activation of a high-gradient magnetic field source (right), or application of a radiofrequency field, the receptor is activated. **D)** Receptor Clustering: Magnetics are bound to receptor complexes. In the absence of a magnetic field (left) the receptors are spaced along the membrane surface. When a field is applied via a high-gradient magnetic needle, the receptors are pulled towards the field source, initiating receptor clustering.<sup>23</sup>



## Conclusions and Future Directions

Magnetic micro- and nanoparticles are increasingly being used in novel and exciting research and clinical applications in biomedicine. Though some of these concepts have been considered for decades, there has been an explosion in this research field since the early 2000s (Figure 6). In addition to the selected applications outlined here, researchers are continually developing imaginative new techniques, such as magnetic levitation for tissue engineering<sup>26</sup> as well as combining magnetics and microfluidics in diagnostic tools.<sup>27</sup> In addition to new applications, the design and synthesis of magnetic micro- and nanoparticles with novel and enhanced properties tailored to specific applications is moving forward at a rapid pace, pointing towards an exciting future for this field.

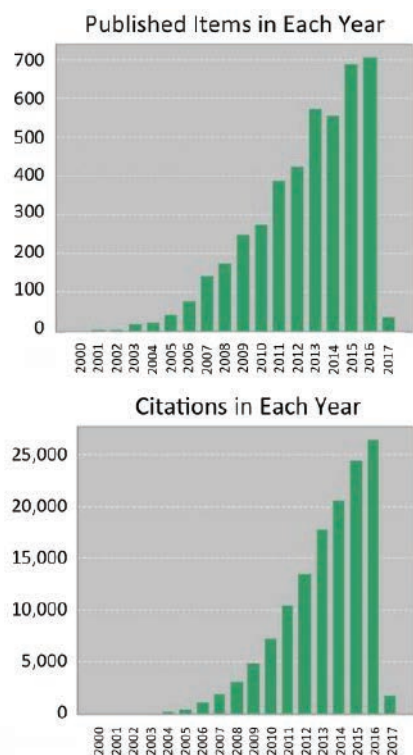


**Figure 6.** Web of Science publication and citation search results for the terms “magnetic + nanoparticle + biomedical”.

## References

- (1) Seifritz, W. *Brit. J. Exper. Biol.* **1924**, *2*, 1–11.
- (2) Heilbrunn, L. V. *Jahrb. Wiss. Bot.* **1922**, *61*, 284.
- (3) Crick, F. H. C.; Hughes, A. F. W. T. *Exp. Cell Res.* **1950**, *1*, 37–80.
- (4) Valberg, P. A.; Albertini, D. F. J. *Cell Biol.* **1985**, *101*, 130–140.
- (5) Wang, N.; Butler, J. P.; Ingber, D. E. *Science*. **1993**, *260*, 1124–1127.
- (6) Sjögren, C. E.; Briley-Saebø, K.; Hanson, M.; Johansson, C. *Magn. Reson. Med.* **1994**, *31*, 268–272.
- (7) Miltenyi, S.; Müller, W.; Weichel, W.; Radburch, A. *Cytometry* **1990**, *11*, 231–238.
- (8) Kozissnik, B.; Dobson, J. *MRS Bull.* **2013**, *38*, 927–931.
- (9) Senyei, A.; Widder, K.; Czerlinski, C. J. *Appl. Phys.* **1978**, *49*, 3578–3583.
- (10) Kyrtatos, P. G.; Lehtolainen, P.; Junemann-Ramirez, M.; Garcia-Prieto, A.; Price, A. N.; Martin, J. F.; Gadian, D. G.; Pankhurst, Q. A.; Lythogoe, M. F. *JACC: Cardiovasc. Interv.* **2009**, *2*, 794–802.
- (11) Yellen, B. B.; Forbes, Z. G.; Halverson, D. S.; Fridman, G.; Barbee, K. A.; Chorny, M.; Levy, R.; Friedman, G. J. *Magn. Magn. Mater.* **2005**, *293*, 647–654.
- (12) Shapiro, B.; Kulkarni, S.; Nacev, A.; Sarwar, A.; Preciado, D.; Depireux, D. *Ann. Rev. Biomed. Eng.* **2014**, *16*, 455–81.
- (13) Mah, C.; Zolotukhin, I.; Fraites, T. J.; Dobson, J.; Batich, C.; Byrne, B. J. *Mol. Ther.* **2000**, *1*(5), S239.
- (14) Mah, C.; Fraites, T. J.; Zolotukhin, I.; Song, S. H.; Flotte, T. R.; Dobson, J.; Batich, C.; Byrne, B. J. *Mol. Ther.* **2002**, *6*(1), 106.
- (15) Plank, C.; Schillinger, U.; Scherer, F.; Bergemann, C.; Rémy, J.-S.; Krötz, F.; Anton, M.; Lausier, J.; Rosenecker, J. *Bio. Chem.* **2003**, *384*, 737–747.
- (16) McBain, S.; Griesenbach, U.; Xenariou, S.; Keramane, A.; Batich, C. D.; Alton, E. W. F. W.; Dobson, J. *Nanotechnology* **2008**, *19*, 405102.
- (17) Hornback, N. B. *Radiol Clin North Am.* **1989**, *27*, 481–488.
- (18) Jordan, A.; Scholz, R.; Wust, P.; Fahling, H.; Felix, R. J. *Magn. Magn. Mater.* **1999**, *201*, 413–419.
- (19) Pankhurst, Q. A.; Connolly, J.; Jones, S. K.; Dobson, J. J. *Phys. D: Appl. Phys.* **2013**, *36*, R167–R181.
- (20) Mérida, F.; Chiu-Lam, A.; Bohórquez, A. C.; Maldonado-Camargo, L.; Eglée Pérez, M.; Pericchi, L.; Torres-Lugo, M.; Rinaldi, C. J. *Magn. Magn. Mater.* **2015**, *394*, 361–371.
- (21) Creixell, M.; Bohórquez, A. C.; Torres-Lugo, M.; Rinaldi, C. *ACS Nano*. **2011**, *5*, 7124–7129.
- (22) Kozissnik, B.; Bohórquez, A. C.; Dobson, J.; Rinaldi, C. *Int. J. Hyperthermia* **2013**, *29*, 706–714(23).
- (24) Dobson, J. *Nat. Nanotechnol.* **2008**, *3*, 139–143.
- (25) Bin, H.; El Haj, A. J.; Dobson, J. *Int. J. Mol. Sci.* **2013**, *14*, 19276–19293.
- (26) Cho, M. H.; Lee, E. J.; Son, M.; Lee, J.-H.; Yoo, D. Kim, J.-W.; Park, S. W.; Shin, J.-S.; Cheon, J. *Nat. Mater.* **2012**, *11*, 1038–1043.
- (27) Souza, G. R.; Molina, J. R.; Raphael, R. M.; Ozawa, M. G.; Stark, D. J.; Levin, C. S.; Bronk, L. F.; Ananta, J. S.; Mandelin, J.; Georgescu, M.-M.; Bankson, J. A.; Gelovani, J. G.; Killian, T. C.; Arap, W.; Pasqualini, R. *Nat. Nanotechnol.* **2010**, *5*, 291–296.
- (28) Pamme, N. *Lab on a Chip* **2006**, *6*, 24–39.

# METHOD: Conjugation Protocols for Magnetic Nanoparticles



Xin Ji, Y. Andrew Wang\*

Ocean NanoTech, LLC  
7964 Arjons Drive, Suite G, San Diego, CA 92126, USA  
\*Email: awang@oceannanotech.com

## Introduction

Metal oxide nanoparticles have generated enormous interest over the past two decades because of their unique size-dependent physical and optical properties.<sup>1-3</sup> Among these nanostructured materials, iron oxide nanoparticles (IONPs) are the most extensively studied nanocrystals. They are noted for their size- and composition-dependent magnetic properties and potential biomedical applications.<sup>1,4</sup> The most successful route to producing high-quality magnetic NPs with controllable size and high crystallinity relies on the high-temperature reaction of organometallic precursors (**Figure 1**). Consequently, any use in bio-inspired studies requires additional chemical manipulation and post-growth surface modification (e.g. ligand exchange or encapsulation) to render the magnetic NPs colloidal stable and biocompatible. These approaches make magnetic NPs amenable for use as contrast enhancement agents in magnetic resonance imaging (MRI), magnetic guidance and separation, and as biological platforms for intracellular imaging, and magnetic carriers for drug-delivery vehicles.<sup>1-5</sup>

An effective integration of controllable biomolecules (e.g., proteins, enzymes, antibodies, drugs, and nucleotides) attached to magnetic NPs must control the ratio of biomolecule per particle, the attachment affinity, the biomolecule orientation, its biocompatibility and colloidal stability, and effective conjugate strategies. Selection of a conjugation method is initially dictated by a combination of factors, including the size and shape of magnetic NPs, the nature of the surface-capping ligands and their available functional groups, the type of biological molecules and their dimension, binding sites, and utility desired in the final application. Those generalized considerations allow nanoparticles to effectively and reproducibly interface with biological systems and be applied in biological targeting, sensing, tracking, and imaging.<sup>6-10</sup>

Most conjugation strategies and immobilization methods for use with magnetic NPs rely on either covalent coupling (including covalent coupling to the nanoparticle surface or surface ligand) or non-covalent interactions (metal coordination or host-guest interactions) (**Figure 2**). Strategies developed over the past decade describe conjugation of nanoparticles with bioactive targets, including carboxyl-to-amine crosslinking using 1-ethyl-3-(3-dimethylaminopropyl)carbodiimide (EDC) and *N*-hydroxysulfosuccinimide (Sulfo-NHS, **Prod. No. 56485**), amine-to-amine via a bis(sulfosuccinimidyl)suberate (BS3) linker, along with amine-to-sulfhydryl crosslinking by using succinimidyl 4-(*N*-maleimidomethyl) cyclohexane-1-carboxylate (SMCC).<sup>11</sup> In addition, a high affinity secondary binding method has also been exploited to assemble bioconjugates via adaptor proteins or metal-polyhistidine conjugation (e.g., NTA-Ni-IONPs to His-tag antibody labeling). Here we provide an overview of several popular bioconjugation approaches and detail the descriptions of standard bioconjugation protocols. These include carbodiimide, avidin-biotin chemistry, crosslinker coupling, or polyhistidine-mediated metal-affinity coordination that are applicable to the most commercially available IONPs functionalized with amine, carboxyl, or streptavidin groups (**Prod. Nos. 747254, 747300, and 900091**).

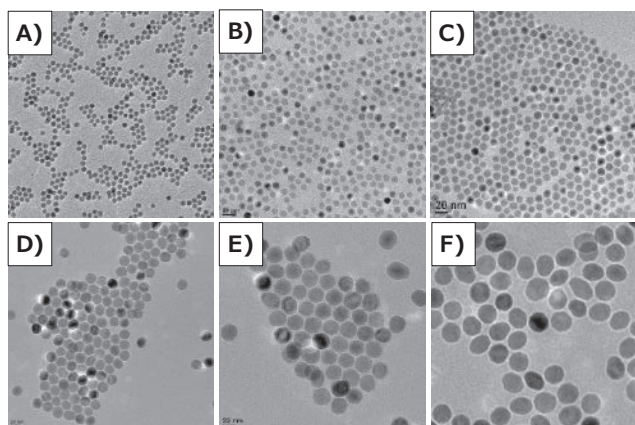


**Figure 1.** Transmission electron microscopy (TEM) images of A) 5 nm, B) 10 nm, C) 15 nm, D) 20 nm, E) 25 nm, and F) 30 nm iron oxide nanoparticles. The TEM images indicate these nanoparticles are monodispersed with uniform cores.

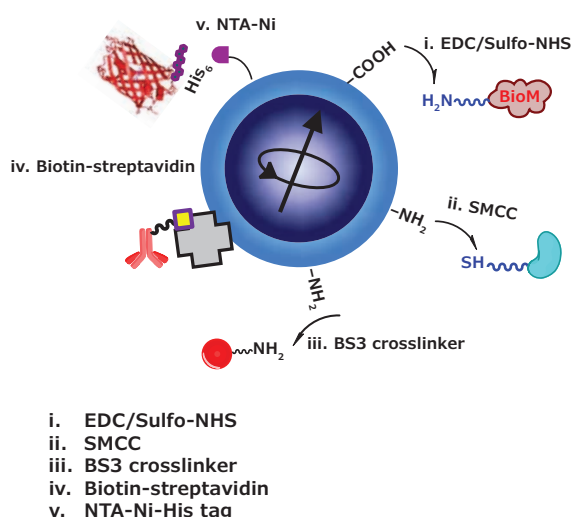


**Figure 2.** Five common chemistries used for creating bioconjugated magnetic NPs.

## Conjugation Protocols

**Note:** Unless otherwise specified, all conjugation protocols presented here refer to IONPs conjugated with antibody/protein/ligands with 50,000 Dalton as an example.

### A. Conjugation of Carboxylic-functionalized Iron Oxide Nanoparticles Using EDC/Sulfo-NHS Chemistry

#### Materials

- Carboxylic functionalized IONPs (Prod. No. **747254**)
- 2 mL microcentrifuge tube (Prod. No. **Z628034**)
- PBS buffer, pH 6.0
- EDC (Prod. No. **E1769**)
- Sulfo-NHS (Prod. No. **56485**)
- PBS buffer, pH 7.4 (Prod. No. **P5493**)
- PD 10 column (Prod. No. **GE17-0851-01**)
- Ethanolamine (Prod. No. **398136**)

#### Procedure

1. Aliquot 0.2 mL of the IONPs functionalized with carboxylic acid group into a 2 mL microcentrifuge tube with 0.1 mL of 0.1 M PBS buffer (pH 6.0).
2. Add 1 mL of 0.1 M PBS buffer (pH 6.0) into the tube containing a pre-weighted mixture of 2 mg EDC and 1 mg Sulfo-NHS, yielding a concentration of 2 mg/mL EDC, and 1 mg/mL Sulfo-NHS. Mix well to ensure solids are completely dissolved.
3. Add 124  $\mu$ L of EDC/Sulfo-NHS solution to the IONP suspension and mix well.
4. React at room temperature for 30 min with continuous mixing on a rotating wheel. Transfer the IONP suspension in a 5 mL reaction tube. Add sufficient 0.1 M PBS buffer (pH 7.4) to make the final volume at 2.5 mL.
5. Transfer 2.5 mL of activated IONPs to the equilibrated PD 10 column to remove excess EDC/Sulfo-NHS. Collect 3.5 mL of eluted IONPs into a 5 mL reaction tube.

6. Add 0.5 mL of 0.1 M PBS buffer (pH 7.4) to the activated IONPs, mix well, and immediately add 0.5 mL targeted antibody/protein/ligands such as protein A, lysine or epidermal growth factor receptor (EGFR) (1 mg/mL in 0.1 M PBS buffer at pH 7.4) to the IONPs.
7. React at room temperature for 3 h with continuous mixing on a rotating wheel.
8. Add 10  $\mu$ L of ethanolamine to the IONP suspension to quench the reaction.
9. Choose a method to purify the conjugated IONPs based on the size of the nanoparticles (**Table 1**).
10. Re-suspend the conjugated IONPs in an appropriate amount of storage buffer (10 mM PBS with 0.02% Na<sub>3</sub>, pH 7.4) depending on the desired concentration.

**Table 1.** Purification Methods for Various Sizes of IONPs.

Particle size (nm)	Purification Methods
5	Spin Column or Ultrahigh Speed Centrifugation (700,000 $\times$ g)
10	Spin Column or Ultrahigh Speed Centrifugation (415,000 $\times$ g)
15	Spin Column or Ultrahigh Speed Centrifugation (330,000 $\times$ g)
20	Spin Column or Magnetic Separation (~12 h separation time)
25	Spin Column or Magnetic Separation (~12 h separation time)
30	Spin Column or Magnetic Separation (~12 h separation time)

### B. Conjugation of Amine-functionalized Iron Oxide Nanoparticles Using Sulfo-SMCC Method

#### Materials

- Amine functionalized IONPs (Prod. No. **747300**)
- 2 mL microcentrifuge tube (Prod. No. **Z628034**)
- PBS buffer pH 7.4 (Prod. No. **P5493**)
- Sulfo-SMCC (Prod. No. **M6035**)
- PD 10 column (Prod. No. **GE17-0851-01**)
- Mercaptosuccinic acid (Prod. No. **88460**)

#### Procedure

1. Aliquot 0.2 mL of the amine-functionalized IONPs (5 mg/mL, total weight nanocrystals plus ligands) into a 2 mL microcentrifuge tube with 0.2 mL of 0.1 M PBS buffer (pH 7.4).
2. Add 0.1 mL of Sulfo-SMCC (10 mg in 1 mL of 0.1 M PBS buffer at pH 7.4) to the IONP suspension.
3. React at room temperature for 1 h with continuous mixing on a rotating wheel. Transfer the IONP suspension in a 5 mL reaction tube. Add sufficient 0.1 M PBS buffer (pH 7.4) to make the final volume 2.5 mL.
4. Transfer 2.5 mL of activated NPs to the equilibrated PD 10 column to remove excess Sulfo-SMCC. Collect 3.5 mL of eluted IONPs into a 5 mL reaction tube.
5. Add 0.5 mL of targeted antibody/protein presenting free thiol groups such as cysteine and methionine (1 mg/mL in 0.1 M PBS buffer at pH 7.4) to the IONPs. React at room temperature for 4 h with continuous mixing.
6. Add 50  $\mu$ L of mercaptosuccinic acid (10 mg/mL in 0.1 M PBS buffer at pH 7.4) to the IONP suspension to quench the reaction.

- Use **Table 1** to select a method to purify the conjugated IONPs based on the size of nanoparticles.
- Re-suspend the conjugated IONPs in an appropriate amount of storage buffer (10 mM PBS with 0.02%  $\text{NaN}_3$ , pH 7.4) depending on the desired concentration.

### C. Conjugation of Amine-functionalized Iron Oxide Nanoparticles Using BS3 Chemistry

#### Materials

- Amine functionalized IONPs (Prod. No. **747300**)
- 2 mL microcentrifuge tube (Prod. No. **Z628034**)
- PBS buffer, pH 7.4 (Prod. No. **P5368**)
- 10 mg BS3 (Prod. No. **S5799**)
- PD 10 column (Prod. No. **GE17-0851-01**)
- Glycine (Prod. No. **50049**)

#### Procedure

- Aliquot 0.2 mL of the IONPs functionalized with amine group (5 mg/mL, total weight nanocrystals plus ligands) into a 2 mL microcentrifuge tube with 0.2 mL of 10 mM PBS buffer (pH 7.4).
- Add 0.1 mL of 10 mg BS3 in 1 mL of 10 mM PBS buffer at pH 7.4 to the IONP suspension.
- React at room temperature for 30 min with continuous mixing on a rotating wheel. Transfer the IONP suspension in a 5 mL reaction tube. Add sufficient 10 mM PBS buffer (pH 7.4) to make the final volume 2.5 mL.
- Transfer 2.5 mL of activated NPs to the equilibrated PD 10 column to remove excess BS3. Collect 3.5 mL of eluted IONPs into a 5 mL reaction tube.
- Add 0.5 mL of targeted antibody/protein/ligand containing amine groups such as protein A, lysine, or EGFR (1 mg/mL in 10 mM PBS buffer at pH 7.4) to the NPs. React at room temperature for 3 h with continuous mixing.
- Add 10  $\mu\text{L}$  of glycine (20 mM) to the IONP suspension to quench the reaction.
- Use **Table 1** to select a method to purify the conjugated IONPs based on the size of nanoparticles.
- Re-suspend the conjugated IONPs in an appropriate amount of storage buffer (10 mM PBS with 0.02%  $\text{NaN}_3$ , pH 7.4) depending on the desired concentration.

### D. Conjugation of Streptavidin-functionalized Iron Oxide Nanoparticles

#### Materials

- Streptavidin functionalized IONPs (Prod. No. **900091**)
- 2 mL microcentrifuge tube (Prod. No. **Z628034**)
- Targeted biotinylated enzyme

#### Procedure

- Aliquot 0.2 mL of the IONPs functionalized with streptavidin (1 mg/mL) into a 2 mL microcentrifuge tube with 0.5 mL of 10 mM PBS buffer (pH 7.4).
- Add 0.2 mL of targeted biotinylated enzyme such as carboxylase (1 mg/mL in 10 mM PBS buffer at pH 7.4) to the IONP suspension. React at room temperature for 3 h with continuous mixing on a rotating wheel.
- Use **Table 1** to select a method to purify the conjugated IONPs based on the size of nanoparticles.
- Re-suspend the conjugated IONPs in an appropriate amount of storage buffer (10 mM PBS with 0.02%  $\text{NaN}_3$ , pH 7.4) depending on the desired concentration.

### E. Conjugation of NTA-Ni-functionalized IONPs




#### Materials

- NTA-Ni functionalized IONPs
- 2 mL microcentrifuge tube (Prod. No. **Z628034**)
- Targeted his-tag antibody

#### Procedure

- Aliquot 0.2 mL of the IONPs functionalized with NTA-Ni (1 mg/mL) into a 2 mL microcentrifuge tube with 0.5 mL of 10 mM PBS buffer (pH 7.4).
- Add 0.2 mL of targeted His-tag antibody (1 mg/mL in 10 mM PBS buffer at pH 7.4) to the IONP suspension. React at room temperature for 3 h with continuous mixing on a rotating wheel.
- Use **Table 1** to select a method to purify the conjugated IONPs based on the size of nanoparticles.
- Re-suspend the conjugated IONPs in an appropriate amount of storage buffer (10 mM PBS with 0.02%  $\text{NaN}_3$ , pH 7.4) depending on the desired concentration.

**Table 2.** Comparison of different purification methods applied to magnetic NP conjugates.

Methods	Instrument or Device	Advantages	Disadvantages
Magnetic Separator		<ul style="list-style-type: none"> <li>✓ Keep stability</li> <li>✓ High recovery</li> </ul>	<ul style="list-style-type: none"> <li>✗ Long purification time for small particles</li> <li>✗ Be suitable for IONPs with 10 nm or above diameter</li> </ul>
Desalting Column		<ul style="list-style-type: none"> <li>✓ Low cost</li> <li>✓ Easy preparation</li> <li>✓ Rapid processing</li> </ul>	<ul style="list-style-type: none"> <li>✗ Single use only</li> <li>✗ Not suitable for large volume</li> <li>✗ Dilute sample concentration</li> </ul>
Centrifugal Filter Device		<ul style="list-style-type: none"> <li>✓ Low cost</li> <li>✓ Concentrated</li> </ul>	<ul style="list-style-type: none"> <li>✗ Single use only</li> <li>✗ Particle may stick on the membrane</li> <li>✗ May reduce colloidal stability</li> </ul>
Dialysis		<ul style="list-style-type: none"> <li>✓ Low cost</li> <li>✓ Easy preparation</li> </ul>	<ul style="list-style-type: none"> <li>✗ Long processing time</li> <li>✗ Low efficiency</li> <li>✗ Sample loss due to leaks</li> </ul>
Ultracentrifuge		<ul style="list-style-type: none"> <li>✓ Universal method</li> </ul>	<ul style="list-style-type: none"> <li>✗ High instrument cost</li> <li>✗ A risk of aggregation</li> </ul>
Stirred Cell		<ul style="list-style-type: none"> <li>✓ Keep stability</li> <li>✓ Large volume</li> </ul>	<ul style="list-style-type: none"> <li>✗ Not suitable for small amount of samples</li> </ul>

## Purification

The properties of the target biomolecules affect purification, and often problems with purification are more difficult to solve than conjugation problems. Any given purification problem will require its own measures. **Table 2** summarizes six common techniques for the purification of IONP conjugates with comparative advantages and limitations.

### A. Magnetic Separator

The magnetic separator is designed for the rapid separation of magnetic NPs in small volumes. Separation time may vary from a few hours to a couple of days, depending on the magnetic strength, particle size, and concentration of magnetic nanocrystals in the solution.

### B. Desalting Column

Size-exclusion chromatography using a desalting column can remove unconjugated biomolecules and separate excess crosslinking or labeling reagents from conjugates.

### C. Centrifugal Filter Device

Centrifugal filter devices offer rapid sample concentration, high recoveries, buffer exchange, and removal of salts and free ligands. The unconjugated biomolecules/linkers can be removed by applying two to three rounds of concentration and dilution

through the membrane filtration device. Molecular weight cut-off (MWCO), membrane material, nanoparticle-bioconjugate stability, and spin time and speed must be considered when using this approach.

### D. Dialysis

Dialysis can be applied as a post treatment for IONPs in an aqueous solution to achieve a high degree of purity. Nanoparticles that cannot pass through the pores of the membrane remain in the dialysis bag, while small molecules freely diffuse across the membrane to the buffer medium.

### E. Ultracentrifugation

Ultracentrifugation is a universal, high-speed method optimized for nanoparticles. It is the easiest way to remove free molecules in the nanoparticle solution. The centrifugation force should be adjusted based on the size of magnetic NPs used.

### F. Stirred Cell

Stirred cells are ideal for concentration, diafiltration, purification, and buffer exchange of NP-conjugate dispersions, including proteins, enzymes, antibodies, and drugs in large volume samples. Gas pressure is applied directly to the cell. Solutes above the MWCO are retained in the cell, while water and solutes below the cut-off pass into the filtrate and out of the cell.

## Characterization

Measuring the change in the hydrodynamic size of a particle before and after conjugation with a protein is a simple way to verify conjugation; however, instrumentation to measure particle size is not widely available in most labs. Gel electrophoresis can be used to measure the change in size and surface charge of NPs before and after bioconjugation. This method works particularly well for negatively charged iron oxide nanoparticles. Unconjugated nanoparticles with a carboxylic acid group migrate particularly faster than conjugated nanocrystals. However, most amine-modified NPs have a neutral surface charge, and the change in migration using gel electrophoresis is not as large before and after conjugation with a protein. Immunoassay tests, such as lateral flow immunoassays with protein A or G on a membrane or dot blot can provide quick and quantitative information to determine if proteins on the surface of the particle have maintained their functionality. The Bradford protein assay can quantify the amount of protein on the particle. Using this method, both total and unreacted protein can be measured; however, protein on the particles surface can't be measured because of strong absorption of iron oxide nanoparticles in the visible range. Another method to quantify antibodies on the particle surface is by the immunofluorescent labeling method,

**Table 3.** Several techniques for validating bioconjugation.

Method	Mechanism	Advantage	Disadvantage
Electrophoresis	Based on the change of size and surface charge of the NPs	Fast, easy operation	Non-quantitative
Immunoassay strip	Antibody on the NPs interacts with protein G on the membrane surface	Easy, fast, functional information	Select appropriate test strips
Bradford protein assay	Reactioned protein = total protein - unreacted protein	Total reaction protein on the beads	No interaction on protein function
Fluorescent dye	Immunofluorescent labeling protein on the NPs	Quantitative	Complicated procedures require standard curve
Hydrodynamic size	Size change	Simple and easy	Not suitable for small molecules

in which dye labeled 2<sup>nd</sup> antibody interacts with primary antibody on the NPs. **Table 3** summarizes the advantages and disadvantages of each characterization method.

## Conclusion

We have summarized a few of the most-used conjugation approaches, optimal working conditions, and purification and characterization methods for use with magnetic NPs. The utility of magnetic NPs in biology and medicine fields requires effective control over their interactions with biological systems. Such control depends, to a large extent, on conjugating nanoprobe to target molecules such as antibodies, proteins, peptides, nucleic acids, and drugs. Apart from the importance of surface ligands that provide nanoparticles hydrophilicity and tunable functional groups, the effectiveness of conjugation strategies used for assembling magnetic NP bioconjugates is essential for successful applications of these materials.

## References

- (1) Yang, J.; Gunn, J.; Dave, S. R.; Zhang, M.; Wang, Y. A.; Gao, X. *Analyst* **2008**, *133*(2), 154.
- (2) Yang, L.; Mao, H.; Wang, Y. A.; Cao, Z.; Peng, X.; Wang, X.; Duan, H.; Ni, C.; Yuan, Q.; Adams, G.; Smith, M. Q.; Wood, W. C.; Gao, X.; Nie, S. *Small* **2009**, *5*, 235.
- (3) Yang, L.; Peng, X. H.; Wang, Y. A.; Wang, X.; Cao, Z.; Ni, C.; Karna, P.; Zhang, X.; Wood, W. C.; Gao, X.; Nie, S.; Mao, H. *Clin. Cancer Res.* **2009**, *15*, 4722.
- (4) Duan, H.; Kuang, M.; Wang, X.; Wang, Y. A.; Mao, H.; Nie, S. *J. Phys. Chem. C* **2008**, *112*, 8127.
- (5) Chen, H.; Yeh, J.; Wang, L.; Khurshid, H.; Peng, N.; Wang, A. Y.; Mao, H. *Nano Res.* **2010**, *3*, 852.
- (6) Chen, H.; Wang, L.; Yeh, J.; Wu, X.; Cao, Z.; Wang, Y. A.; Zhang, M.; Yang, L.; Mao, H. *Biomaterials* **2010**, *31*, 5397.
- (7) Peng, X.-H.; Wang, Y.; Huang, D.; Wang, Y.; Shin, H. J.; Chen, Z.; Spewak, M. B.; Mao, H.; Wang, X.; Wang, Y.; Chen, Z.; Nie, S.; Shin, D. M. *ACS Nano* **2011**, *5*, 9480.
- (8) Huang, J.; Wang, L.; Lin, R.; Wang, A. Y.; Yang, L.; Kuang, M.; Qian, W.; Mao, H. *ACS Appl. Mater. Interfaces* **2013**, *5*, 4632.
- (9) Lee, G. Y.; Qian, W. P.; Wang, L.; Wang, Y. A.; Staley, C. A.; Satpathy, M.; Nie, S.; Mao, H.; Yang, L. *ACS Nano* **2013**, *7*, 2078.
- (10) Wang, W.; Ji, X.; Na, H. B.; Safi, M.; Smith, A.; Palui, G.; Perez, J. M.; Mattoussi, H. *Langmuir* **2014**, *30*, 6197.
- (11) Hermanson, G. T. *Bioconjugate Techniques (Third edition)*; Academic Press: Boston, **2013**.

# Recommended Products for Magnetic Imaging-based Diagnostics

For more information on these materials, visit [SigmaAldrich.com/nanopowders](https://www.sigmaaldrich.com/nanopowders).

## Iron Oxide Nanoparticles

Functional Group	Form	Composition	Avg. Part Size (nm) (TEM)	Prod. No.
amine	dispersion	Fe 1 mg/mL in H <sub>2</sub> O	5	747343-10ML
	dispersion	Fe 1 mg/mL in H <sub>2</sub> O	10	747300-10ML
	dispersion	1 mg/mL in H <sub>2</sub> O	15	900199-10ML
	dispersion	1 mg/mL in H <sub>2</sub> O	25	900028-10ML
	dispersion	Fe 1 mg/mL in H <sub>2</sub> O	30	747327-10ML
biotin	dispersion	Fe 1 mg/mL in H <sub>2</sub> O	5	747416-1ML
	dispersion	1 mg/mL (in 10 mM PBS buffer)	15	900037-1ML
	dispersion	1 mg/mL (in 10 mM PBS buffer)	25	900038-1ML
	dispersion	Fe 1 mg/mL in H <sub>2</sub> O	30	747432-1ML
carboxylic acid	dispersion	Fe 5 mg/mL in H <sub>2</sub> O	5	797146-2ML
	dispersion	Fe 5 mg/mL in H <sub>2</sub> O	10	747254-2ML
	dispersion	5 mg/mL in H <sub>2</sub> O	15	900201-2ML
	dispersion	5 mg/mL in H <sub>2</sub> O	25	900200-2ML
	dispersion	Fe 5 mg/mL in H <sub>2</sub> O	30	747335-2ML
dextran	dispersion	10 mg/mL in H <sub>2</sub> O	5	900147-2ML
N-succinimidyl ester	powder	Fe ~1.25 % (w/w)	5	747440-1G
	powder	Fe ~1.25 % (w/w)	10	747459-1G
	powder	Fe ~1.25 % (w/w)	15	900041-1G
	powder	-	25	900034-1G
	powder	Fe ~1.25 % (w/w)	30	747467-1G
PEG	dispersion	Fe 1 mg/mL in H <sub>2</sub> O	5	790508-10ML
	dispersion	Fe 1 mg/mL in H <sub>2</sub> O	10	747319-10ML
	dispersion	1 mg/mL in H <sub>2</sub> O	15	900026-10ML
	dispersion	1 mg/mL in H <sub>2</sub> O	25	900027-10ML
	dispersion	Fe 1 mg/mL in H <sub>2</sub> O	30	747408-10ML
rhodamine B	dispersion	1 mg/mL in H <sub>2</sub> O	10	900146-2ML
streptavidin	dispersion	1 mg/mL in H <sub>2</sub> O	10	900091-1ML
	dispersion	1 mg/mL in H <sub>2</sub> O	15	900092-1ML
	dispersion	1 mg/mL in H <sub>2</sub> O	20	900093-1ML
	dispersion	1 mg/mL in H <sub>2</sub> O	25	900094-1ML
	dispersion	1 mg/mL in H <sub>2</sub> O	30	900148-1ML
-	dispersion	5 mg/mL in chloroform	5	900082-5ML
	dispersion	5 mg/mL in chloroform	10	900084-5ML
	dispersion	5 mg/mL in toluene	15	900063-5ML
	dispersion	5 mg/mL in H <sub>2</sub> O	15	900043-5ML
	dispersion	5 mg/mL in chloroform	15	900083-5ML
	dispersion	5 mg/mL in chloroform	20	900088-5ML
	dispersion	5 mg/mL in H <sub>2</sub> O	25	900042-5ML
	dispersion	5 mg/mL in toluene	25	900064-5ML
	dispersion	5 mg/mL in chloroform	25	900089-5ML
	dispersion	5 mg/mL in H <sub>2</sub> O	30	900062-5ML
	dispersion	5 mg/mL in toluene	30	900081-5ML
	dispersion	5 mg/mL in chloroform	30	900090-5ML

# Fluorescent Nanoparticles for Imaging and Diagnostics



Maria Ada Malvindi,<sup>1</sup> Enrico Binetti,<sup>1</sup>  
Pier Paolo Pompa<sup>1,2,\*</sup>

<sup>1</sup>HiQ-Nano Srl, Via Barsanti, 73010,  
Arnesano (Lecce), Italy

<sup>2</sup>Istituto Italiano di Tecnologia, Italy

\*Email: info@hiqnano.com

## Introduction

In the last decade, fluorescent nanomaterials have demonstrated enormous potential to advance biomedical applications and have provided a deeper understanding of biology and medicine at the molecular level.<sup>1</sup> Fluorescence imaging of cells using either dyes or nanoparticles (NPs) is now among the most widespread methods in biology. Fluorescent NPs sidestep some of the problems inherent to fluorescent dyes based on organic molecules such as low-intensity emission, non-specific binding, and undesired sequestration. In addition, unlike classical dyes, fluorescent NPs guarantee longer *in situ* stability and photostability while maintaining their original optical properties upon interaction with target biomolecules. However, an important limitation of many fluorescent NPs is their cytotoxicity, as in the case of cadmium-based quantum dots. In this regard, the development of silica-based fluorescent nanoparticles shows considerable value. Bright silica nanoparticles have proven to be an excellent material for chemical incorporation and doping with molecular species to enhance their functionality, while guaranteeing long-term biocompatibility. Moreover, because of their unique properties, these NPs have been successfully applied in diagnostics, cancer therapeutics, and gene and drug delivery. The silica NPs offer the following features:

- Ability to adsorb and carry various compounds, such as drugs, oligonucleotides, and proteins
- Low toxicity
- Biodegradability
- Ease of surface functionalization
- Large cellular uptake
- Wide tunability range (from 10 to several hundred nm), while maintaining high monodispersity (**Figure 1**)
- Ability to incorporate a large number of dye molecules within the silica matrix to yield NPs with varying excitation and emission wavelengths with orders of magnitude higher brightness than organic fluorophores (**Figure 2**)

The encapsulation of fluorophores within a silica matrix tremendously enhances their chemical stability and prevents photobleaching, which makes them suitable for sensitive biomedical applications.

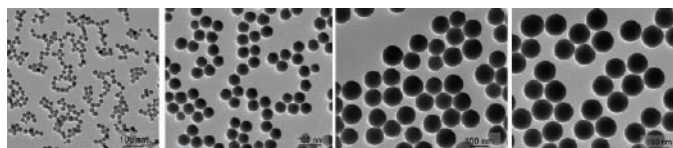


**Figure 1.** Monodispersed fluorescent silica nanobeads of different sizes. From left to right: 25 nm (Prod. No. **797901**), 50 nm (Prod. No. **797952**), 90 nm (Prod. No. **797944**), and 120 nm (Prod. No. **797871**).

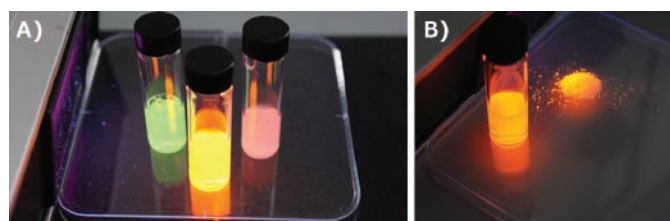


**Figure 2.** Multicolor fluorescent silica nanobeads dispersed in water and lyophilized form. Emission wavelength of the nanobeads can be tuned from blue to red and infrared.

## Bioconjugation and Applications of Fluorescent Silica Nanoparticles

The creation of multifunctional nanoparticles through the integration of optical and chemical properties in a single NP has increased the use of fluorescent NPs in advanced biophysical applications. The presence of a high silanol concentration on the surface of fluorescent silica NPs facilitates a wide variety of surface reactions, including the binding of biomolecules. Several strategies and a variety of surface treatments are available for equipping nanoparticles with the functional groups required for convenient conjugation to biological molecules. Functional groups, such as amines, carboxyls, and thiols can be introduced to the NP surface through the addition of an additional silica coating layer containing the desired functional group. Alkoxysilanes are frequently used as the functionalization molecules; carboxyethylsilanetriol, for example, is used for the introduction of carboxylic acid groups, 3-aminopropyltriethoxysilane for amino groups, and



(3-mercaptopropyl) trimethoxysilane for thiol groups. Once the NPs have been modified with functional groups, a wide range of molecules can be conjugated to them, including low molecular weight molecules such as folic acid,<sup>2</sup> peptides (RGD, antigenic peptides, and internalization peptides),<sup>3</sup> proteins (BSA, transferrin, antibodies, lectins, cytokines, fibrinogen, and thrombin),<sup>4</sup> polysaccharides (hyaluronic acid, chitosan, dextran),<sup>5</sup> DNA,<sup>6</sup> plasmids,<sup>7</sup> siRNA,<sup>8</sup> and miRNA.<sup>9</sup> These bioconjugations can be achieved either through standard covalent bioconjugation schemes, such as carbodiimide chemistry, succinimidyl ester hydrolysis chemistry, disulfide-coupling chemistry, or through electrostatic interactions between NPs and charged molecules. A strong covalent bond between the biomolecule and the functionalized NP surface is usually preferred for several reasons. Covalent bonds avoid non-specific adsorption and desorption at the NP surface, not only ensuring precise control of the biological moieties, but also allowing for the tuning of the amount and orientation of the immobilized molecules. **Figure 3** shows some typical procedures used for the bioconjugation of fluorescent silica nanoparticles.

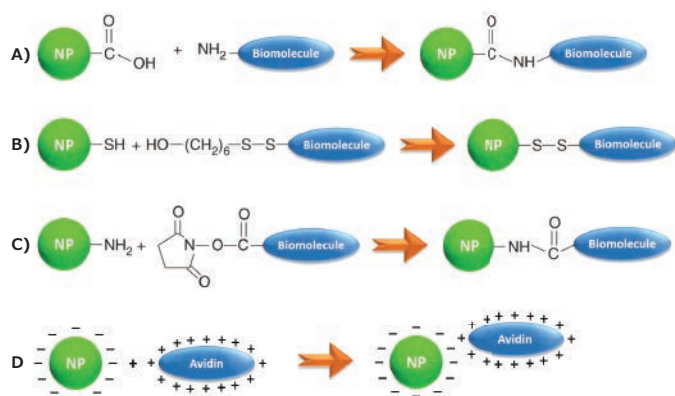


**Figure 3.** Strategies used to produce various nanobioconjugates, by linking the NPs with a variety of biomolecules.

Surface functionalization allows fluorescent silica NPs to be conjugated with a large variety of biological molecules. Carboxyl-modified fluorescent silica NPs (**Figure 3A**) are suitable for covalent bonding with antibodies or other amine-containing biomolecules via water-soluble carbodiimide reagents.<sup>10</sup> Disulfide-modified peptides can be immobilized onto thiol-functionalized NPs by disulfide-coupling chemistry (**Figure 3B**).<sup>11</sup> Amine-modified NPs (**Figure 3C**) can be coupled to a wide variety of drugs via succinimidyl esters.<sup>12</sup> Alternatively, charged NPs, either positive or negative, can be exploited for electrostatic interactions with oppositely charged molecules (**Figure 3D**).<sup>13</sup>

The introduction of appropriate functional groups on fluorescent silica NPs and subsequent conjugation to biomolecules makes them suitable for use in the detection of single molecules and bioimaging, as well as for the delivery of nucleic acids. This is important because it provides a new way to treat genetic diseases, overcoming the obstacles associated with current gene delivery systems, such as the poor intracellular uptake,

instability, and the non-specific immune stimulation. Fluorescent silica NPs represent an excellent nanomaterial for advanced applications in this field. These NPs satisfy three essential conditions:

- Strong affinity with nucleic acids, permitting high gene loading through electrostatic interaction between genes and the NP surface.
- Efficient gene release, allowing delivery of the genes directly to the target.
- Potential for intracellular tracking: the high and stable NP fluorescence allows optical monitoring of intracellular trafficking and gene transfection (**Figure 4**).

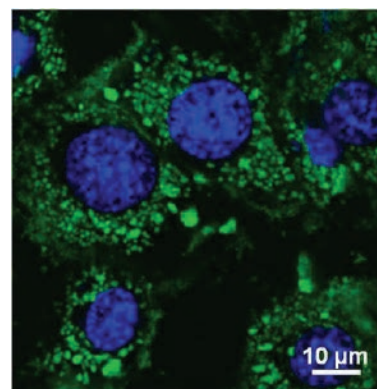


**Figure 4.** Confocal microscopy image of 120 nm fluorescent nanobeads (Prod. No. 797863) internalized by A549 cells.

The electrostatic binding between oligonucleotides and amino-modified NPs represents the most commonly used strategy for the functionalization of NPs with DNA. Functionalized silica NPs display a positive surface charge at neutral pH, enabling simple DNA trapping via electrostatic interaction. Fluorescent silica NPs can thus efficiently transport siRNA<sup>15</sup> and antisense oligonucleotides, which inhibit gene expression at both mRNA and protein levels.<sup>14</sup> Flow cytometry and confocal microscopy are able to track fluorescent silica NPs during transfection, confirming the delivery of nucleic acids into target cells.<sup>16</sup> The ability to adsorb genes onto the fluorescent NP surface allows for the controlled and efficient delivery to targeted tissues, while minimizing systemic side effects and toxicity. Moreover, the high fluorescence and photostability of fluorescent silica NPs allows for the detection of gene products down to sub-femtomolar concentrations,<sup>17</sup> making these NPs a highly efficient probe in bioanalysis.

Diagnostics is a further application that is well-suited for functionalized silica NPs. The covalent immobilization of primary or secondary antibodies onto a NP surface enables highly selective and efficient binding to cancer cells, making the direct observation of pathological samples feasible and allowing for immediate diagnosis. Indeed, antibodies provide fluorescent NPs with highly specific targeting properties, enhancing cellular

uptake, improving site-specific drug release, and activating several immunological pathways that can lead to increased anticancer effect. Hybrid fluorescent NPs are also able to boost the detection capabilities of conventional flow cytometry. It has been observed that fluorescent silica NPs can increase the detection sensitivity of cancer cells by about 100-fold, compared to traditional dye-labeled antibodies.<sup>18</sup> Fluorescent NPs decorated with antibodies against cell membrane receptors, receptor ligands, and recognition peptides are proving very useful reagents for cell imaging. Different types of targets, including proteins,<sup>19</sup> cells, such as SmIgG+B lymphocyte for the immunodiagnosis of systemic erythema lupus,<sup>20</sup> and bacteria<sup>21</sup> have been detected by using these NPs.

## Conclusions

In this micro review, we described different bioconjugation strategies of fluorescent silica NPs and the subsequent advantages for their application in advanced diagnostics and imaging. In particular, we focused on the adsorption of DNA on the NP surface and on the covalent conjugation of antibodies. The reported examples demonstrated that fluorescent silica NPs represent a versatile tool for the development of efficient bioimaging probes for both *in vitro* and *in vivo* applications. Bioconjugated fluorescent NPs exhibited unique advantages by virtue of their size, stability, biocompatibility, and optical properties. As robust and bright light emitters, fluorescent silica NPs have been adopted as a new class of fluorescent labels, finding application as multifunctional nanoplatforms for both diagnostic and therapeutic purposes for the development of personalized healthcare.

## References

- (1) Reisch, A.; Klymchenko, A. S. *Small* **2016**, *12*, 1968.
- (2) Wang, X.; Morales, A. R.; Urakami, T.; Zhang, L.; Bondar, M.; Komatsu, M.; Belfield, K. D. *Bioconjugate Chem.* **2011**, *22*, 1438.
- (3) Fang, I. J.; Slowing, I. I.; Wu, K. C. W.; Lin, V. S. Y.; Trewyn, B. G. *Chem. - Eur. J.* **2012**, *18*, 7787.
- (4) Foldbjerg, R.; Wang, J.; Beer, C.; Thorsen, K.; Sutherland, D. S.; Autrup, H. *Chem. Biol. Interact.* **2013**, *204*, 28.
- (5) Salis, A.; Fantì, M.; Medda, L.; Nairi, V.; Cugia, F.; Piludu, M.; Sogos, V.; Monduzzi, M. *ACS Biomater. Sci. Eng.* **2016**, *2*, 741.
- (6) Torney, F.; Trewyn, B. G.; Lin, V. S. Y.; Wang, K. *Nat. Nano.* **2007**, *2*, 295.
- (7) Kneuer, C.; Sameti, M.; Haltner, E. G.; Schiestel, T.; Schirra, H.; Schmidt, H.; Lehr, C. M. *Int. J. Pharm.* **2000**, *196*, 257.
- (8) Xia, T.; Kovochich, M.; Liong, M.; Meng, H.; Kabehie, S.; George, S.; Zink, J. I.; Nel, A. E. *ACS Nano.* **2009**, *3*, 3273.
- (9) Gandhi, N. S.; Tekade, R. K.; Chougule, M. B. *J. Control. Release.* **2014**, *194*, 238.
- (10) Liu, S.; Zhang, H. L.; Liu, T. C.; Liu, B.; Cao, Y. C.; Huang, Z.-L.; Zhao, Y. D.; Luo, Q. M. *J. Biomed. Mater. Res. A.* **2007**, *80A*, 752.
- (11) Hilliard, L. R.; Zhao, X.; Tan, W. *Anal. Chim. Acta.* **2002**, *470*, 51.
- (12) Doussineau, T.; Trupp, S.; Mohr, G. J. *J. Colloid. Interf. Sci.* **2009**, *339*, 266.
- (13) Schiestel, T.; Schirra, H.; Gerwann, J.; Lesniak, C.; Kalaghi-Nafchi, A.; Sameti, M.; Borchard, G.; Haltner, E.; Lehr, C. M.; Schmidt, H. *Mater. Res. Soc. Proc.* **1998**, *65*.
- (14) Rejeeth, C.; Salem, A. *J. Pharm. Pharmacol.* **2016**, *68*, 305.
- (15) Meng, H.; Liong, M.; Xia, T.; Li, Z.; Ji, Z.; Zink, J. I.; Nel, A. E. *ACS Nano.* **2010**, *4*, 4539.
- (16) Gemeinhart, R. A.; Luo, D.; Saltzman, W. M. *Biotechnol. Prog.* **2005**, *21*, 532.
- (17) Zhao, X.; Tapeç-Dytioco, R.; Tan, W. *J. Am. Chem. Soc.* **2003**, *125*, 11474.
- (18) Estévez, M. C.; O'Donoghue, M. B.; Chen, X.; Tan, W. *Nano Res.* **2009**, *2*, 448.
- (19) Deng, T.; Li, J. S.; Jiang, J. H.; Shen, G. L.; Yu, R. Q. *Adv. Funct. Mater.* **2006**, *16*, 2147.
- (20) He, X.; Wang, K.; Tan, W.; Li, J.; Yang, X.; Huang, S.; Li, D.; Xiao, D. *J. Nanosci. Nanotechnol.* **2002**, *2*, 317.
- (21) Tan, W.; Wang, K.; He, X.; Zhao, X. J.; Drake, T.; Wang L.; Bagwe, R. P. *Med. Res. Rev.* **2004**, *24*, 621.

# Method: Fluorescent Silica Nanoparticle Bioconjugation

Maria Ada Malvindi,<sup>1</sup> Enrico Binetti,<sup>1</sup>  
Pier Paolo Pompa<sup>1,2</sup>

<sup>1</sup>HiQ-Nano Srl, Via Barsanti, 73010,  
Arnesano (Lecce), Italy

<sup>2</sup>Instituto Italiano di Tecnologia, Italy

\*Email: info@hiqnano.com

The conjugation of fluorescent silica nanoparticles (SiO<sub>2</sub>NPs) with biomolecules can be performed in different ways. We focus here on two strategies: adsorption of biomolecules through electrostatic interactions and covalent bonding through 1-ethyl-3-(3-dimethylaminopropyl)carbodiimide (EDC) chemistry. Using monodispersed and stable NPs with well-defined chemical-physical properties (e.g., size, shape, surface charge, and stability) facilitates the functionalization process and allows elevated control over the number and orientation of attached biomolecules. It is helpful to characterize the NPs at each modification step to have direct control over functionalization.

## Fluorescent Silica Nanoparticle Functionalization with DNA

The functionalization of fluorescent silica nanoparticles (**Prod. No. 797952**) with oligonucleotides, plasmids, and siRNA is possible through molecular adsorption on the nanoparticle surface. The adsorption of biomolecules on a nanoparticle occurs via electrostatic interaction between differently charged moieties. Before the adsorption of DNA, NPs are functionalized with amine groups in order to create a positively charged surface that will interact with negatively charged DNA molecules (**Figure 1**). Generally, the silane 3-aminopropyltriethoxysilane (APTES) is most frequently used to introduce NH<sub>2</sub> on the NP surface. After the functionalization, it is advisable to characterize the NPs using Z-Potential measurements to confirm that the surface charge has changed from negative to positive. DNA-functionalized fluorescent NPs can be used in several applications, such as imaging, diagnostics, and gene and drug delivery.

### Adsorption of DNA on Fluorescent SiO<sub>2</sub>NPs



**Figure 1.** Electrostatic adsorption of DNA molecules on amine-modified fluorescent Silica NPs.

## Materials

- Fluorescent SiO<sub>2</sub>NPs (See full product list at end of this section)
- Acetic acid (**Prod. No. 45726**)
- APTES (**Prod. No. 440140**)
- TBE (45 mM Tris, 45 mM boric acid, and 1 mM EDTA)
- 1% agarose gel
- SYBR® Green dye (**Prod. No. L6544**)

## Protocol

1. Prepare 3 microtubes with 100 µg of fluorescent SiO<sub>2</sub>NPs each. One aliquot can be used as a control, whereas the other 2 can be used to test the adsorption of different amount of oligonucleotides, plasmid vectors, RNA, or DNA.
2. Disperse NPs in 1 mL of 1 mM acetic acid and sonicate for 5 minutes in a sonicator bath, or until the NPs are completely redispersed.
3. Add 50 µL of APTES to the NPs solution to introduce -NH<sub>2</sub> groups to the NPs surface.
4. Stir for 1 hour at room temperature.
5. Precipitate NPs by centrifuging for 30 minutes at 4,200 × g.
6. Remove the supernatant and add 1 mL of water.
7. Repeat steps 5–6 four times to ensure any excess of APTES is removed.
8. Verify the change in NP surface charge from negative to positive through the measurement of Z-Potential using a Zetasizer (**Figure 2**).
9. Precipitate the NPs in the three microtubes by centrifuging for 30 minutes at 4,200 × g.
10. Remove the supernatant and disperse 3 NP aliquots in TBE (45 mM Tris, 45 mM boric acid, and 1 mM EDTA).
11. To quantify the DNA binding capability of the amino-functionalized NPs, add increasing amounts of oligonucleotides (0.5 and 2 µg)<sup>1,2</sup> to the two aliquots and incubate for 2 hours. The third aliquot of NPs is used as a control.
12. After incubation, load the mixture of NPs and DNA (**Figure 3**, columns 2, 3) on a 1% agarose gel in TBE buffer containing SYBR® Green dye. Also, load two control samples in the gel: the amine modified NPs (**Figure 3**, column 4) and oligonucleotide (**Figure 3**, column 1).

13. After 40 minutes (100 V) of electrophoresis, view the gel on a UV transilluminator and quantify the DNA using a gel documentation system (Figure 3). A thicker band of unbound DNA is seen in the column where the ratio of DNA to NPs is higher (Figure 3, column 3).
14. Choose the DNA concentration to be used in your NP functionalization by evaluating the gel and the NPs dispersion in solution. The presence of NP aggregates in solution indicates an excessive amount of DNA was used during the functionalization step (step 11).
15. Verify the NP-to-DNA surface charge change with the measurement of Z-Potential (Figure 4).
16. Store NPs functionalized with DNA at 4 °C before use.

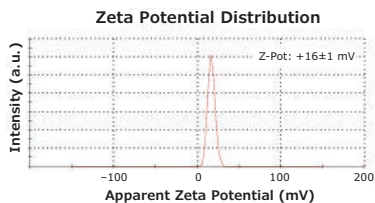


**Figure 2.** Z-Potential of amine modified fluorescent SiO<sub>2</sub>NPs. The positive NPs surface charge confirms the NPs amine modification.

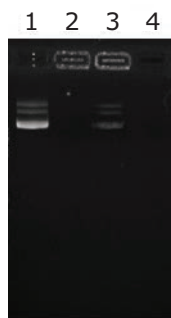


**Figure 3.** Representative gel showing the migration patterns of two quantities of DNA (0.5 and 2 µg) mixed with 100 µg of 50 nm amine-modified fluorescent SiO<sub>2</sub>NPs after 40 minutes (100 V) of electrophoresis. **Column 1:** DNA; **Column 2:** fluorescent SiO<sub>2</sub>NPs mixed with 0.5 µg of DNA; **Column 3:** fluorescent SiO<sub>2</sub>NPs mixed with 2 µg of DNA; **Column 4:** 50 nm amine-modified fluorescent SiO<sub>2</sub>NPs.

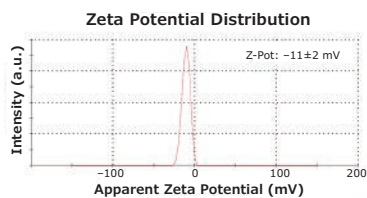


**Figure 4.** Z-Potential of fluorescent SiO<sub>2</sub>NPs mixed with 0.5 µg of DNA. The negative NPs surface charge confirms the adsorption of DNA on NPs surface.

## Fluorescent Silica NPs Functionalization with Antibodies

The functionalization of fluorescent silica nanoparticles with antibodies is possible through the formation of an amide bond between the carboxylated fluorescent silica NPs and the amino groups of the antibodies, using 1-ethyl-3-(3-dimethylaminopropyl) carbodiimide hydrochloride (EDC) as

### Covalent Binding of Antibody on Fluorescent SiO<sub>2</sub>NPs



**Figure 5.** Covalent binding of Antibody molecules on carboxyl-modified fluorescent Silica NPs.

the crosslinking agent. The procedure below outlines steps for modifying the surface of fluorescent silica with carboxyl groups and to covalently bind with an antibody. NPs are first modified with amine groups and then treated with succinic anhydride to attach carboxyl groups. These NPs are then activated with EDC and NHS and incubated with an antibody (Figure 5). The procedure allows conjugation of carboxyl groups with the amine groups of the Fc region, and therefore preserves the full functionality of the antibody as it leaves the antigen-binding site (Fab region) free for targeting. The NPs are characterized at each step of functionalization through Zeta Potential and DLS.

### Materials

- Fluorescent SiO<sub>2</sub>NPs (Prod. No. **797952**)
- Acetic acid (Prod. No. **45726**)
- APTES (Prod. No. **440140**)
- Succinic anhydride in dimethylformamide
- EDC (Prod. No. **E1769**)
- NHS (Prod. No. **130672**) BSA

### Protocol

1. Weigh 2 mg of fluorescent SiO<sub>2</sub>NPs.
2. Disperse NPs in 1 mL of 1 mM acetic acid and sonicate for 5 minutes in a sonicator bath, or until the NPs are completely redispersed.
3. Add 100 µL of APTES to the NPs solution to introduce -NH<sub>2</sub> groups to the NP surface.
4. Stir for 1 hour at room temperature.
5. Precipitate NPs by centrifuging for 30 minutes at 4,200 × g.
6. Remove the supernatant and add 1 mL of water.
7. Repeat steps 5–6 four times to be sure that the excess of APTES is removed.
8. Verify the change in NP surface charge from negative to positive through the measurement of Z-Potential using a Zetasizer (Figure 6).
9. Precipitate the NPs by centrifuging for 30 minutes at 4,200 × g.
10. Remove supernatant and disperse NPs in 10% succinic anhydride in dimethylformamide (DMF) and stir for 24 hours.
11. Precipitate the NPs by centrifuging for 30 minutes at 4,200 × g.
12. Remove the supernatant and add 1 mL of water.
13. Repeat steps 11–12 four times to ensure the excess succinic anhydride is removed.
14. Verify the change in NP surface charge from positive to negative by measuring Z-Potential using a Zetasizer (Figure 7A).
15. Measure the size through dynamic light scattering (DLS) (Figure 7B) to ensure that NPs are well dispersed.
16. Add 10 mM EDC and 10 mM NHS to activate carboxyl groups for 1 hour.

17. Add 30  $\mu\text{g}$  of antibody to the activated NPs and incubate for 3 hours.
18. After incubation, wash the antibody conjugated NPs with water three times and dissolve in 2 mL of water.
19. Measure NPs surface charge using a Zetasizer (**Figure 8A**) to confirm the proximity of the charge measured at step 14.
20. Measure the size through dynamic light scattering (DLS) (**Figure 8B**) to ensure that NPs are well dispersed. An increase in particle size is expected.
21. Add 0.1% BSA.
22. Store NPs functionalized with antibody at 4  $^{\circ}\text{C}$  before use.

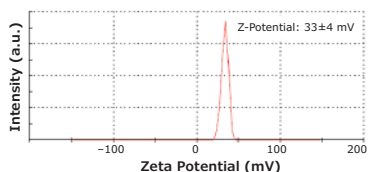


**Figure 6.** Z-Potential of amine modified fluorescent  $\text{SiO}_2$  NPs. The positive NPs surface charge confirms the NPs amine modification.

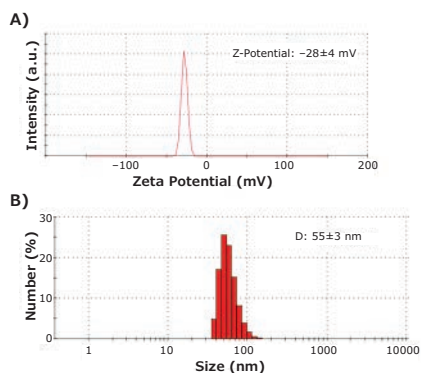


**Figure 7.** A) Z-Potential of carboxyl modified fluorescent  $\text{SiO}_2$  NPs. The negative NPs surface charge confirms the NPs carboxyl modification. B) DLS of carboxyl modified fluorescent  $\text{SiO}_2$  NPs. NPs are well dispersed in water.

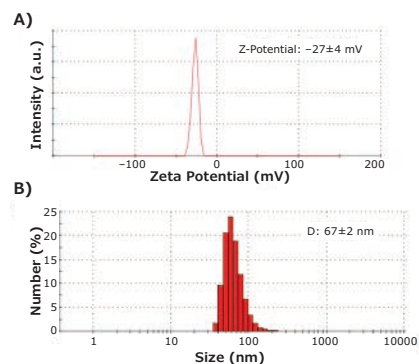


**Figure 8.** A) Z-Potential of Antibody conjugated fluorescent  $\text{SiO}_2$  NPs. The conjugation of antibody on NPs surface does not induce a significant change of NPs surface charge. B) DLS of Antibody conjugated fluorescent  $\text{SiO}_2$  NPs. The increase in size may be attributed to the conjugation of the antibodies on the particle's surface.

## References

- (1) Malvindi, M. A.; Brunetti, V.; Vecchio, G.; Galeone, A.; Cingolani, R.; Pompa, P. P. *Nanoscale*. **2012**, *4*, 486.
- (2) Bardi, G.; Malvindi, M. A.; Gherardini, L.; Costa, M.; Pompa, P. P.; Cingolani, R.; Pizzorusso, T. *Biomaterials*. **2010**, *31*, 6555.

# Recommended Products for Diagnostics Using Fluorescence Techniques

For more information on these materials, visit [SigmaAldrich.com/biomedical](http://SigmaAldrich.com/biomedical).

## Fluorescent Silica Nanoparticles

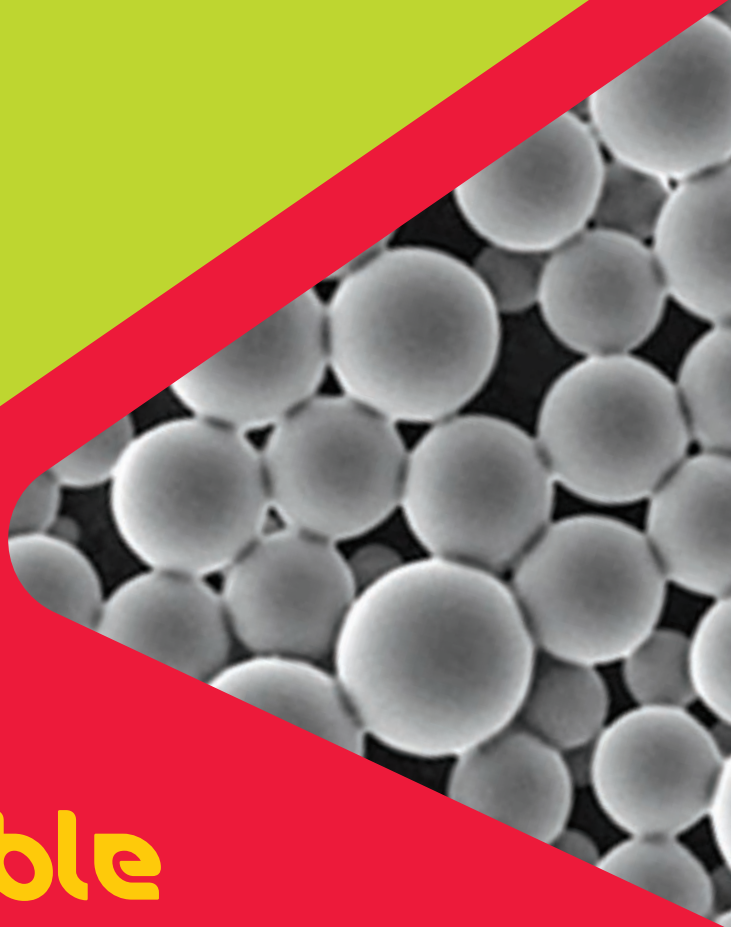
Name	Particle Size (nm)	Emission Max (nm)	Absorption Max (nm)	Prod. No.
Fluorescent silica nanobeads	25	590	570	797928-5MG
	50	590	570	797936-5MG
	90	590	570	797898-5MG
	120	590	570	797863-5MG
Ultrastable fluorescent silica nanobeads	25	590	570	797901-2MG
	50	590	570	797952-2MG
	90	590	570	797944-2MG
	120	590	570	797871-2MG

## Silica Nanospheres

Name	Particle Size (nm)	Concentration	Prod. No.
Silica nanospheres	50	10 % (w/v) in ethanol	803073-1ML
	80	10 % (w/v) in ethanol	803197-1ML
	100	10 % (w/v) in ethanol	803308-1ML
	120	10 % (w/v) in ethanol	803405-1ML
	140	10 % (w/v) in ethanol	803510-1ML
	160	10 % (w/v) in ethanol	803634-1ML
	180	10 % (w/v) in ethanol	803731-1ML
	200	10 % (w/v) in ethanol	803847-1ML

## Monodispersed Nanodiamonds

Surface Group	Zeta Potential (mV)	Particle Size (nm) (DSL)	Concentration	Prod. No.
carboxylated	+45.1 ±20%	5	10 mg/mL in ethylene glycol	900184-5ML
	+35.5 ±20%	5	10 mg/mL in NMP	900177-5ML
	+31.1 ±20%	5	10 mg/mL in H <sub>2</sub> O	900180-5ML
	+45.1 ±20%	5	10 mg/mL in polyalphaolefin synthetic base oil	900178-5ML
hydroxylated	+34.5 ±20%	5	10 mg/mL in DMSO	900179-5ML
-	+56.0 ±20%	5	10 mg/mL in DMSO	900185-5ML



# Biodegradable Drug Delivery

## PLGA Microspheres and Nanoparticles

Degradex® poly(D,L-lactide-co-glycolide) (PLGA) microspheres and nanoparticles are a compelling choice for a variety of drug delivery applications including:

- Particle compatibility testing prior to active pharmaceutical ingredient (API) loading
- Surface-conjugated drug carriers for the covalent attachment of proteins, peptides, antibodies, or antigens
- Imaging and diagnostic applications with fluorescent Degradex® particles
- Particle size standards for instrument calibration

Name	Particle Size (Average diameter)	Product number
PLGA nanoparticles	100 nm	805092
	500 nm	805149
PLGA microspheres	2 µm	805130
	50 µm	805122
Green fluorescent PLGA nanoparticles	100 nm	805157
	500 nm	805300
Green fluorescent PLGA microspheres	2 µm	805181
	50 µm	805165

Learn more about Degradex® PLGA particles and their applications at:

**[SigmaAldrich.com/biodegradable](https://SigmaAldrich.com/biodegradable)**

# Plasmonic Materials and Their Applications in Diagnostics



Bo Zhang,<sup>1</sup> Jeyarama S. Ananta,<sup>1</sup> Meijie Tang,<sup>1</sup> Hongjie Dai<sup>1,2,\*</sup>

<sup>1</sup>Nirmidas Biotech, Inc.  
2458 Embarcadero Way, Palo Alto, CA 94303, USA

<sup>2</sup>Department of Chemistry  
Stanford University, William Keck Science Building, Stanford, CA 94305-5080

\*Email: hdai1@stanford.edu

## Introduction

Surface plasmons are delocalized electron oscillations that exist at the interface between two media.<sup>1</sup> Metal-air interfaces are the most thoroughly studied surface-plasmon systems.<sup>2</sup> Triggered by an electromagnetic wave (e.g., light), delocalized electron oscillations create local electric fields (**Figure 1**). The surface plasmon and related phenomena have been used in various applications in the past two decades, especially with great success in protein-interaction measurement for diagnostics.<sup>1</sup>

Different strategies have been developed for using surface plasmons in biosensing applications:

1. Surface-plasmon-resonance (SPR) technology for measurement of biomolecule absorption
2. Plasmonic nanomaterials as optical labels for biomolecule detection
3. Surface-enhanced Raman spectroscopy (SERS)
4. Surface-plasmon-enhanced fluorescence technology

Currently, SPR is the most mature biosensing technology, but other approaches are emerging that require less complicated instrumentation and offer higher sensitivity. Different plasmonic materials, ranging from thin gold films to plasmonic-nanoparticle and single-plasmonic-nanoparticle assemblies, are synthesized and engineered for different biosensing strategies. Sandwich immunoassay structures are usually applied for surface-plasmon-based biosensing where plasmonic materials either serve as signal-transducing labels (strategies 1 and 2) or as signal-enhancing substrates (strategies 3 and 4). Surface-plasmon-based biosensing technologies are able to measure various types of biomolecules, including proteins, peptides, lipids, small molecules, DNA, and RNA. By measuring such molecules, surface plasmon-based biosensing is capable of assisting in diagnostics of infectious diseases, autoimmune diseases, inflammatory diseases, cardiovascular diseases, cancer, etc. The following sections focus on the four biosensing strategies using surface plasmons.<sup>1</sup>

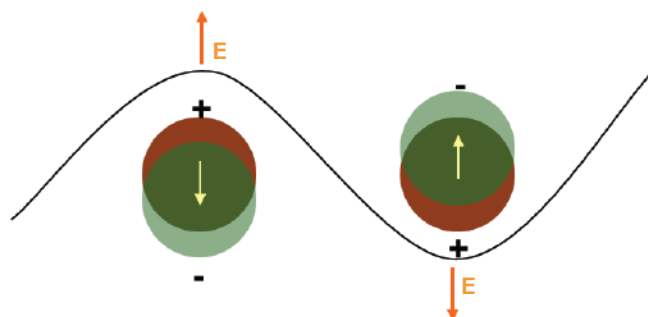


**Figure 1.** Schematic diagram of surface plasmons triggered by an electromagnetic wave.

## Surface-Plasmon-Resonance (SPR) Technology

Surface-plasmon-resonance (SPR) technology is the most well-established biosensing technology based on surface plasmons. SPR captures protein targets as it detects variation in the reflectance properties of the surface of a sensor coated with probe protein.<sup>1</sup> A beam of polarized light is directed through a prism onto a noble metal (e.g., gold) film and reflected toward a light-collecting sensor. At a unique incident beam angle, the film reaches maximum surface plasmon resonance and this incident light is significantly absorbed as the electromagnetic energy transforms into surface plasmons (**Figure 2**). The angle depends on the wavelength of light, properties of the metal film, and protein absorption. Protein probes immobilized on the gold film capture target proteins and cause observable change of this angle, thus enabling measurement of the target protein.

Unlike other immunoassays, the SPR immunoassay does not require a label because the signal transduction results from the absorption of protein on the gold film. SPR immunoassays can also be applied to measure antigen-antibody reaction rates, given



that the absorption caused angle shift is a dynamic process. Recently, localized-surface-plasmon resonance (LSPR) with plasmonic nanoparticles has also been implemented for sensitive biomolecular detection.<sup>3,4</sup> Compared to SPR, LSPR confines surface plasmons in a nanoparticle of size comparable or smaller than the wavelength of light used to excite the plasmon. SPR and LSPR have similar advantages and limitations, while the considerably shorter field decay length for LSPR (5–6 nm) over SPR (100 nm) makes LSPR less sensitive to interference from refractive index fluctuations, but more sensitive to changes on the surface, leading to higher biosensing sensitivity.

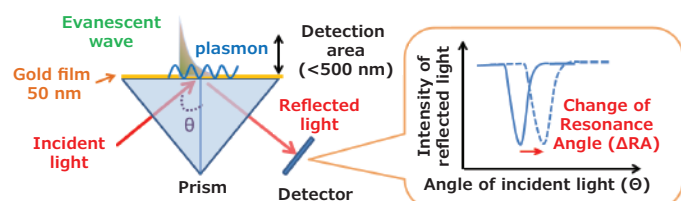


**Figure 2.** Schematic diagram of the surface plasmon resonance mechanism.<sup>5</sup>

## Plasmonic Nanomaterials as Optical Labels for Biomolecule Detection

Incident light can cause collective oscillation of conduction electrons in plasmonic nanoparticles, with a resonant frequency that relates to the shape, size, and elemental composition of the nanoparticles. The light absorption and scattering by the plasmonic nanoparticles can be a million times greater than fluorescent molecules.<sup>6</sup> This advantage was facilitated by the adoption of plasmonic nanoparticles as signal transduction agent for immunoassays. For example, Roberto de la Rica and Molly Stevens introduced a plasmonic gold-nanoparticle-formation mechanism for ultrasensitive prostate-specific antigen (PSA) and HIV-1 capsid antigen p24 detection using the enzyme-linked immunosorbent assay (ELISA) system (**Figure 3**).<sup>7</sup> Chad Mirkin et al. used plasmonic nanoparticles together with an oligonucleotide-amplification system for ultrasensitive detection of PSA.<sup>8</sup>

## Surface-enhanced Raman Spectroscopy (SERS)

Since its discovery in the 1970s, surface-enhanced Raman scattering (SERS) has proven to be a powerful technique capable of intensifying the emission of extremely weak inelastic scattering of molecules (**Figure 4**).<sup>9</sup> In fact, SERS has been demonstrated to enhance the Raman scattering intensities significantly enough to allow detection of even a single Raman-active molecule.<sup>10,11</sup> Fundamentally, the oscillating electric field of incident light in a SERS experiment couples to the inherent conduction electron oscillation (plasmon) of a metal, thereby creating a resonance that drives plasmon oscillation. The oscillation increases the local electric field and thus the field experienced by a nearby Raman-active molecule. SERS has various applications in biomolecular detection. For example, Van Duyne et al. applied silver film over polystyrene latex

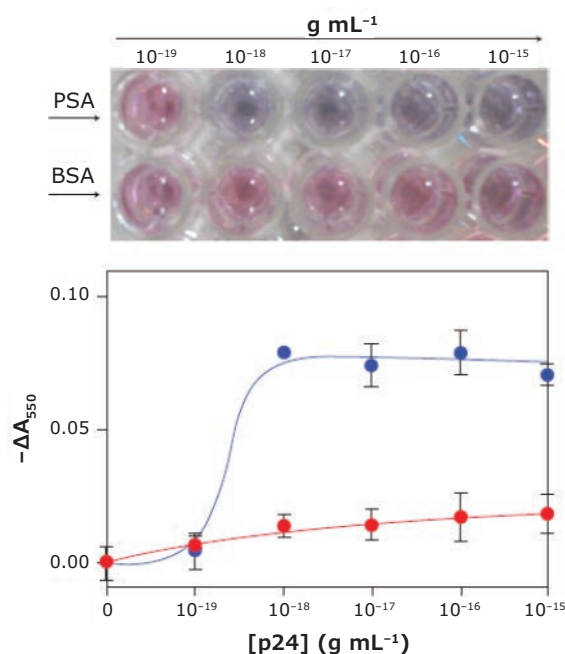


**Figure 3.** Sensitive p24 detection using plasmonic gold nanoparticles as a label.<sup>7</sup>

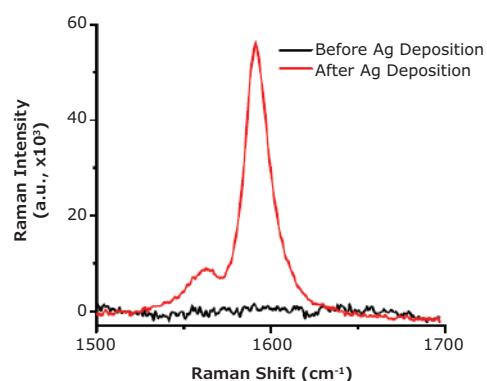
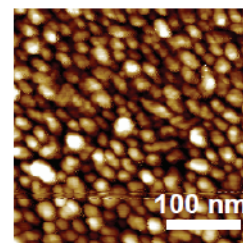


**Figure 4.** Deposition of an Ag film onto single-walled nanotubes to yield a SERS effect. Top: AFM images of Ag film covering single-walled nanotubes. Bottom: single-walled nanotube g-band Raman spectra collected from SWNTs labeling an immunoassay before (black) and after Ag deposition (red). A ~50 fold enhancement was observed<sup>14</sup>.

nanospheres as a SERS substrate for a glucose biosensor.<sup>12</sup> Porter et al. reported the detection of a pancreatic cancer marker MUC4 using SERS technology.<sup>13</sup> Tabakman et al. reported SERS detection of carcinoembryonic antigen down to the 1 femtomolar (fM) range.<sup>14</sup>

## Surface Plasmon-enhanced Fluorescence Technology

Due to the wide implementation of fluorescence-based biosensing technology, surface plasmon enhanced fluorescence technology can be more easily deployed than SERS. Compared to SERS, the effect of plasmon modes of metal on fluorescence emission is more complex, with experimental observation demonstrating both fluorescence quenching and enhancement effects from metal surfaces.<sup>15</sup> It was demonstrated that plasmon enhanced fluorescence arises both from the significantly enhanced local electric field generated by surface plasmons as well as by the increased radiative decay rate of fluorophores at excited states due to plasmon resonance.<sup>15</sup> As there are various types of fluorescence-based diagnostic technologies, fluorescence enhancement afforded by plasmonic materials could significantly improve sensitivity and lead to improved diagnostics using less sample and time.

It has been demonstrated that plasmonic gold slides (pGOLD™) (Figure 5) that afford near-infrared fluorescence enhancement (NIR-FE) of up to 100-fold (Figure 5C), yield fM detection limits for protein analytes in serum<sup>16</sup> over a dynamic range spanning as many as or more than six orders of magnitude.<sup>16</sup> pGOLD is able to provide fluorescence enhancement for assays based on widely used fluorescence scanners, requiring no change to common laboratory procedures.

In contrast to chemical amplification made common by ELISA, fluorescence enhancement in this case is accomplished physically, through the interaction of both the excitation field and the fluorescence emission dipole coupling to a plasmonic,

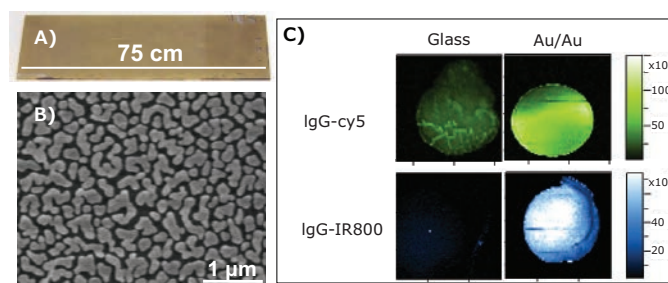


**Figure 5.** Characterization and NIR-fluorescence enhancement of pGOLD. **A)** Digital photograph of pGOLD slide. **B)** Scanning electron micrograph of the plasmonic gold film from (A) showing the nano-island structures. **C)** Fluorescence enhancement of dye-labeled IgG directly dried onto glass compared to pGOLD. Cy<sup>5</sup> and IR800 fluorescence are shown on a fixed scale and both are enhanced on pGOLD slides.

nanoscale gold film. This means the plasmonic protein chip methodology requires no additional procedural steps or expensive reagents, and yet provides a vastly improved signal-to-background ratio for immunoassays. It is crucial to produce gold films with desired nanostructured morphologies to achieve optimal NIR-FE, as most metal films on substrates would cause quenching, and undesired reduction in signal-to-background ratio. Here, the unique morphology of the nanoscale gold film supports localized surface plasmon resonances efficiently at re-radiation and scattering, rather than absorption, providing enhanced optical properties of fluorescent and Raman-scattering contrast agents. Antibody arrays have been successfully established on pGOLD for sensitive detection of cancer biomarkers and cytokines (Figure 6),<sup>16</sup> outperforming widely used nitrocellulose slides and functionalized glass slides. Antigen

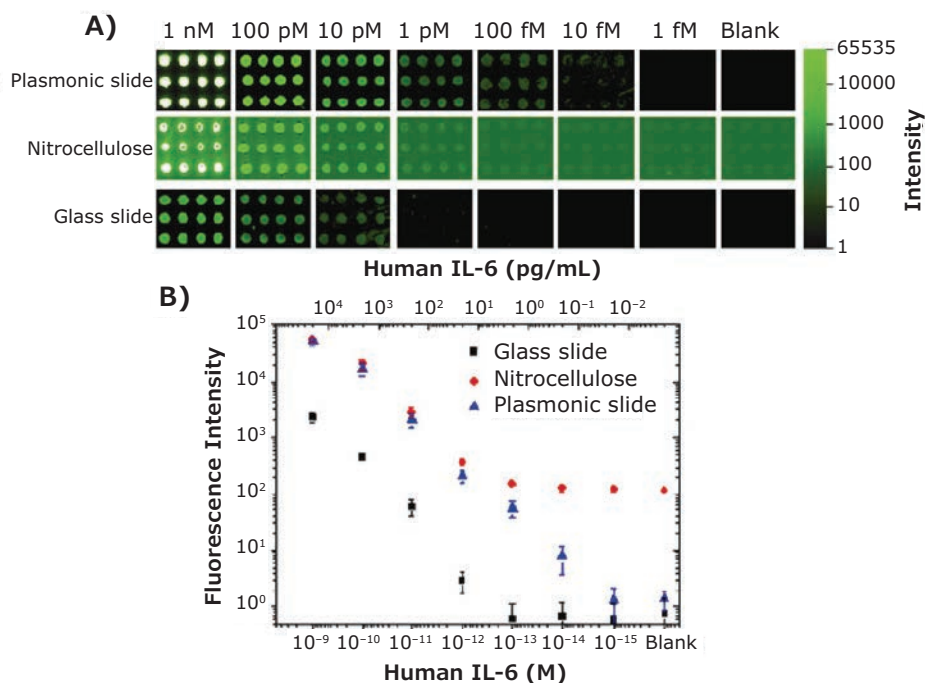


**Figure 6.** Antibody-based cytokine microarray assays on a pGOLD slide, a nitrocellulose slide, and a glass slide. **A)** NIR fluorescence images for Cytokine IL-6 detection using a microarray on a pGOLD slide, a nitrocellulose slide, and a conventional glass slide. **B)** Standard curves for IL-6 quantification on the three substrates.<sup>20</sup>

arrays were developed on pGOLD with multicolor detection of IgG/IgM/IgA antibody subtypes in type 1 diabetes and toxoplasmosis,<sup>17,18</sup> with results matching those of reference labs by conventional methods including the dye-test.<sup>17,18</sup> It has also been demonstrated that plasmonic gold coated microspheres can be used to enhance protein detection sensitivity by flow cytometry.<sup>19</sup> Plasmonic silver slides have been demonstrated to enhance the fluorescence with wider wavelength coverage (500 nm–NIR region).

## Conclusions

Plasmonic materials have emerged as one of the most important tools for biomolecular detection in clinical diagnostics. This review summarizes recent research and trends in plasmonic materials and their use for clinical diagnostics, aiming to achieve biosensing with high sensitivity, multiplexity, and low cost. Plasmonic materials are easy to fabricate, and they enable a vast signal boost for different signal transduction modalities. They hold great promise for addressing clinical diagnostic needs.

## References

- (1) Homola, J. *Chem. Rev.* **2008**, *108*, 462–493.
- (2) Homola, J.; Yee, S. S.; Gauglitz, G. *Sens. Actuat B-Chem.* **1999**, *54*, 3–15.
- (3) McFarland, A. D.; Van Duyne, R. P. *Nano Lett.* **2003**, *3*, 1057–1062.
- (4) Haes, A. J.; Chang, L.; Klein, W. L.; Van Duyne, R. P. *J. Am. Chem. Soc.* **2005**, *127*, 2264–2271.
- (5) Yanase, Y.; Hiragun, T.; Ishii, K.; Kawaguchi, T.; Yanase, T.; Kawai, M.; Sakamoto, K.; Hide, M. *Sensors (Basel)*. **2014**, *14*, 4948–4959.
- (6) Schultz, S.; Smith, D. R.; Mock, J. J.; Schultz, D. A. *P. Natl. Acad. Sci. USA.* **2000**, *97*, 996–1001.
- (7) de la Rica, R.; Stevens, M. M. *Nat. Nanotechnol.* **2012**, *7*, 821–824.
- (8) Nam, J. M.; Thaxton, C. S.; Mirkin, C. A. *Science.* **2003**, *301*, 1884–1886.
- (9) Fleischmann, M.; Hendra, P. J.; Mc Quillan, A. J. *Chem. Phys. Lett.* **1974**, *26*, 163–166.
- (10) Nie, S. M.; Emery, S. R. *Science.* **1997**, *275*, 1102–1106.
- (11) Kneipp, K.; Wang, Y.; Kneipp, H.; Perelman, L. T.; Itzkan, I.; Dasari, R.; Feld, M. S. *Phys. Rev. Lett.* **1997**, *78*, 1667–1670.
- (12) Shafer-Peltier, K. E.; Haynes, C. L.; Glucksberg, M. R.; Van Duyne, R. P. *J. Am. Chem. Soc.* **2003**, *125*, 588–593.
- (13) Wang, G.; Lipert, R. J.; Jain, M.; Kaur, S.; Chakraborty, S.; Torres, M. P.; Batra, S. K.; Brand, R. E.; Porter, M. D. *Anal. Chem.* **2011**, *83*, 2554–2561.
- (14) Tabakman, S. M.; Chen, Z.; Casaloungue, H. S.; Wang, H.; Dai, H. *Small.* **2011**, *7*, 499–505.
- (15) Aslan, K.; Gryczynski, I.; Malicka, J.; Matveeva, E.; Lakowicz, J. R.; Geddes, C. D. *Curr. Opin. Biotechnol.* **2005**, *16*, 55–62.
- (16) Tabakman, S. M.; Lau, L.; Robinson, J. T.; Price, J.; Sherlock, S. P.; Wang, H.; Zhang, B.; Chen, Z.; Tangsombotvisit, S.; Jarrell, J. A.; Utz, P. J.; Dai, H. *Nat. Commun.* **2011**, *2*, 466.
- (17) Zhang, B.; Kumar, R. B.; Dai, H.; Feldman, B. J. *Nat. Med.* **2014**, *20*, 948–953.
- (18) Li, X.; Pomares, C.; Gonfrier, G.; Koh, B.; Zhu, S.; Gong, M.; Montoya, J. G.; Dai, H. *J. Clin. Microbiol.* **2016**, *54*, 1684–1685.
- (19) Zhang, B.; Yang, J.; Zou, Y.; Gong, M.; Chen, H.; Hong, G.; Antaris, A.; Li, X.; Liu, C.; Chen, C.; Dai, H. *Chem. Sci.* **2014**, *5*, 4070–4075.
- (20) Zhang, B.; Price, J.; Hong, G.; Tabakman, S. M.; Wang, H.; Jarrell, J. A.; Feng, J.; Utz, P. J.; Dai, H. *Nano Res.* **2014**, *6*, 113–120.

**Sigma-Aldrich**<sup>®</sup>  
Lab Materials & Supplies

# polymers with possibilities

## PEGs for Drug Delivery

### Polymer of choice for optimal and reproducible results.

When it comes to drug delivery technologies and solutions, poly(ethylene glycol)s or PEGs are the polymer of choice for optimal and reproducible results. With excellent pharmacokinetic properties, they are ideal materials for bioconjugation, pegylation, crosslinking, and hydrogel formation. Let us help you transform your work into new therapeutic discoveries with our diverse PEG selection.

### Features

- Well characterized, high-purity materials with a wide variety of functional groups
- High biocompatibility, with little to no immunogenicity
- $M_n$  ranging from 1-40 kDa
- Reactivity
  - For amine, N-terminal amine, and thiol pegylation
  - For click chemistry and photochemistry
  - Heterobifunctional and multi-arm PEG crosslinkers
- Narrow polydispersity



For a complete list of available materials, visit:  
[SigmaAldrich.com/PEG](http://SigmaAldrich.com/PEG)

# METHOD: Conjugation of Proteins to Gold Nanoparticles



**Benny Pacheco**

919 Fraser Drive, Unit 11, Burlington, ON L7L 4X8, Canada  
bpacheco@cytodiagnosics.com  
Email: bpacheco@cytodiagnosics.com

## Introduction

The unique optical properties of gold nanoparticle conjugates make them ideal reagents for use in many applications, including use as Surface Enhanced Raman Spectroscopy (SERS) probes, local delivery vehicles of miRNA to tumors, and *in vivo* tracking of cancer-specific T-cells.<sup>1-3</sup> The most prolific application of gold nanoparticles has been their use in lateral flow immunoassays. Lateral flow assays are fast, economical, and well-suited for rapidly growing applications such as point-of-care tests.<sup>4</sup>

Two different strategies—passive adsorption and covalent conjugation—are most commonly used to conjugate ligands such as antibodies, proteins, or enzymes to gold nanoparticles. Passive adsorption is the most straightforward route and is considered the classic method for conjugation. It requires the simple mixing of the ligand under pre-determined optimal conditions (pH and protein concentration) using standard citrate-coated gold nanoparticles. This results in an antibody, protein, or enzyme “passively” bound to the gold surface through a combination of electrostatic interactions and through the high affinity of available free thiols on the protein. Although passive adsorption is very cost effective, the method has several drawbacks. These include desorption of the protein from the gold surface over time, and in some cases, loss of activity due to disturbances in the tertiary structure of the conjugated protein,<sup>5,6</sup> possible impairment of necessary conformational changes required for activity, or shielding of the antigen-binding or active site.

Covalent conjugation negates many of the drawbacks of passive adsorption, making it an excellent alternative. However, covalent binding requires the surface modification of gold nanoparticles to introduce functional groups (e.g., *N*-hydroxysuccinimide (NHS) ester or maleimide groups) to which the ligand of interest can be conjugated. Protocols for the conjugation of an antibody to both NHS- and maleimide-activated gold nanoparticles are outlined in this article. A procedure for the activation of carboxylated gold nanoparticles using EDC/NHS chemistry is also outlined.

For these methods, both passive and covalent conjugation reactions ideally result in a gold conjugate with a high density of the conjugated molecule in which the ligand maintains its functional form, e.g., antigen binding for an antibody conjugate and enzyme activity for an enzyme conjugate. In addition to verifying the successful conjugation of the ligand, it is imperative to perform a functional characterization of the conjugate to ensure optimal performance in downstream applications. For example, antibodies can be assessed using a standard dot-blot test.

## Example Method I: Conjugation of Antibodies to Non-functionalized Gold Nanoparticles Through Passive Adsorption

This method describes a procedure for conjugating a standard IgG antibody to non-functionalized citrate-coated gold nanoparticles (“standard gold nanoparticles”) through passive adsorption. The method is rapid, economical and results in an antibody-gold conjugate with high avidity.

In the procedure described below, the pH and antibody concentration are titrated to quickly identify the optimal conditions where a sufficient amount of antibody passively and strongly adsorbs to saturate the gold surface via electrostatic forces. The optimal pH for conjugation is generally close to or slightly higher than the isoelectric point (pI) of the protein to be conjugated when it has a neutral or a slightly net-negative charge.<sup>7</sup>

### Materials

- Antibody to be conjugated: 5–10 mg/mL in 0.5× Phosphate-Buffered Saline, pH 7.4

**Note:** For effective conjugation, the purity of the protein should be considered. Contaminating proteins such as Bovine Serum Albumin (BSA) may compete with the antibody to be conjugated and hence severely reduce the conjugation efficiency and the performance of the conjugate in downstream applications.

- 5–100 nm non-functionalized citrate-coated gold nanoparticles (OD=1) (See Product Table at the end of this section)
- 10% NaCl
- Protein Dilution Buffer: 0.5× Phosphate-Buffered Saline, pH 7.4 (Prod. No. P5493)
- 10% BSA (w/v)
- Conjugate Storage Buffer: 20 mM Tris, pH 8.0, 150 mM NaCl, 1% BSA (w/v)
- Conjugation Buffers:
  1. 0.1 M Sodium Phosphate, pH 5.7
  2. 0.1 M Sodium Phosphate, pH 6.2
  3. 0.1 M Sodium Phosphate, pH 6.5
  4. 0.1 M Sodium Phosphate, pH 7.0
  5. 0.1 M Sodium Phosphate, pH 7.4
  6. 0.1 M Sodium Phosphate, pH 7.8
  7. 0.1 M Borate, pH 8.2
  8. 0.1 M Borate, pH 8.7
  9. 0.1 M Sodium Phosphate, pH 9.0
  10. 0.1 M Potassium Carbonate, pH 9.2
  11. 0.1 M Potassium Carbonate, pH 9.4
  12. 0.1 M Potassium Carbonate, pH 9.8

### Conjugation Optimization Protocol

1. Prepare a dilution series (n=7) of the protein using the protein dilution buffer. A good starting range for most proteins is in the range of 0.15–4 mg/mL, see **Table 1**.
2. Add 4 µL of conjugation buffer stock solutions 1–12 to each well in corresponding columns 1–12 of a 96 well plate according to grid system as shown in **Table 1**.
3. Add 100 µL of gold nanoparticles stock to each well. Mix thoroughly by pipetting up and down several times.
4. Transfer 2 µL from each individual protein dilution prepared in step 1 to corresponding wells (Row A–H) according to the example grid system in **Table 1**. Mix well by pipetting up and down several times.
5. Incubate for 15 minutes at room temperature.
6. Add 100 µL of 10% NaCl to each well in row B–H (wells in row A are control wells for each pH).
7. Incubate for 15 minutes at room temperature.
8. Read the absorbance at 530 nm and 690 nm using a plate reader.
9. Calculate the ratio of the absorbance at 690 nm over 530 nm for each well and determine the net change between sample wells (row B–H) and control wells (row A) as indicated in the formula below.

$$\text{Ratio} = \left( \frac{\text{Abs}@690_{\text{sample}}}{\text{Abs}@530_{\text{sample}}} \right) - \left( \frac{\text{Abs}@690_{\text{control}}}{\text{Abs}@530_{\text{control}}} \right)$$

10. The optimal pH and protein concentration can be found in the samples where no significant aggregation is induced upon addition of NaCl.

Aggregation is indicated by an increased absorbance at 690 nm and reduced absorbance at 530 nm. The optimal conjugation conditions are thus found where the net-change in the 690 nm/530 nm ratio between a sample (e.g., well D5) and its corresponding control well (e.g., well D1) is close to zero. Plotting the calculated net-changes as shown in **Figure 1B** makes it straightforward to find optimal conditions for conjugation.

Optimal conditions can also be determined by simply observing the plate with the naked eye since no major change in color should be observed in the samples where conjugation is optimal when compared to that of the control. Sub-optimal conditions on the other hand will result in the gold nanoparticles turning blue/purple or losing color altogether (**Figure 1A**).

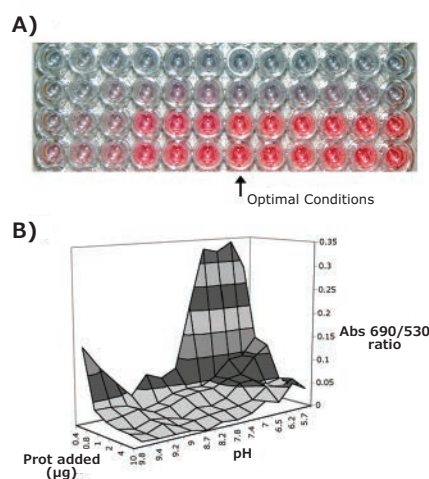


**Figure 1.** Typical results obtained after addition of NaCl (Example Method I—step 6). As seen in **A**) optimal conditions are indicated by wells where visually no change in color is observed, or in more detail **B**) where the net change in the 690 nm/530 nm ratio between a sample and that of a control is close to zero.

### Conjugation Reaction Protocol (10 mL reaction)

1. Adjust the pH of 10 mL gold nanoparticle solution as determined during the optimization procedure above by adding 400 µL of conjugation buffer with the corresponding pH and mix thoroughly.
2. Add the pH-adjusted gold nanoparticle solution to 200 µL of antibody in protein dilution buffer with a concentration as determined during the optimization procedure above.
3. Incubate with mixing for 30 minutes at room temperature.
4. Add 0.5 mL of 10% BSA and mix thoroughly.
5. Transfer the conjugate into 1.5 mL microcentrifuge tubes and centrifuge at the proper speed for the particular gold nanoparticle size, see **Table 2** at the end of this method.
6. Carefully remove and discard the supernatant.
7. Resuspend gold conjugate pellets in a total volume of 1 mL of conjugate storage buffer.
8. Measure the optical density with a UV/Vis spectrophotometer and adjust to desired concentration.
9. Store at 2–8 °C until further use.

## Example Method II: Conjugation of Antibodies to Carboxylated Gold Nanoparticles

This example protocol describes the covalent coupling of a standard full-length IgG antibody to carboxylated gold nanoparticles via an intermediate activation step in which the carboxyl group is converted into a primary amine-reactive *N*-hydroxysuccinimide ester (NHS).

### Materials

- Antibody to be conjugated: 0.5–5 mg/mL (see **Table 3** at the end of this method) in 1× Phosphate Buffered Saline (PBS), pH 7.4

**Note:** For effective conjugation, the purity of the protein should be considered. Any other molecules containing primary amines (e.g., TRIS) or other contaminating proteins (e.g., BSA) will compete with the protein to be conjugated and severely reduce the conjugation efficiency.

- 5–100 nm Carboxylated gold nanoparticles (OD=50) (See Product Table at the end of this section)
- Activation Buffer: 10 mM 2-(*N*-morpholino)ethanesulfonic acid (MES), pH 5.5
- Coupling Buffer: 1× Phosphate Buffered Saline (PBS), pH 7.4 (**Prod. No. P5493**)
- Washing Buffer: 1× Phosphate Buffered Saline (PBS), pH 7.4, 0.05% TWEEN® 20 (w/v)
- Conjugate Storage Buffer: 20 mM Tris (pH 8.0), 150 mM NaCl, 1% BSA (w/v)
- 1-Ethyl-3-[3-dimethylaminopropyl]carbodiimide hydrochloride (EDC) (**Prod. No. E1769**)
- *N*-hydroxysulfosuccinimide (Sulfo-NHS) (**Prod. No. 56485**)

### NHS-activation Protocol

1. Dissolve 60 mg of EDC in 500  $\mu$ L of activation buffer.
2. Dissolve 72 mg of Sulfo-NHS in 500  $\mu$ L of activation buffer.
3. Mix the EDC and Sulfo-NHS solution together to obtain a final concentration of 30 mg/mL and 36 mg/mL of EDC and Sulfo-NHS, respectively.
4. Transfer 10  $\mu$ L of carboxylated gold nanoparticles into a microcentrifuge tube.
5. Add 10  $\mu$ L of the EDC/NHS solution prepared in step 3 to the carboxylated gold nanoparticles.
6. Incubate for 30 minutes at room temperature.
7. Add 1 mL of washing buffer and mix thoroughly.
8. Centrifuge the vial using a speed suitable for the particular gold nanoparticle size that you are working with, see **Table 2**.
9. Remove supernatant and immediately proceed to conjugate your protein, see conjugation protocol below.

### Conjugation Protocol

1. Transfer 10  $\mu$ L of antibody solution to the activated gold nanoparticles prepared above and mix thoroughly.

**Note:** Sonication can help at this stage to re-solubilize the gold nanoparticles.

2. Incubate for 2 hours at room temperature

3. Add 1 mL of washing buffer and mix thoroughly.
4. Centrifuge the vial using a speed suitable for the particular gold nanoparticle size that you are working with, see **Table 2**.
5. Remove supernatant.
6. Resuspend the pellet with 50  $\mu$ L of conjugate storage buffer.
7. Measure the optical density using a UV/Vis spectrophotometer and adjust to desired concentration using conjugate storage buffer.
8. Store the gold conjugate at 2–8 °C until further use.

## Example Method III: Conjugation of Antibodies to NHS-activated Gold Nanoparticles

This example protocol describes the covalent coupling of a standard IgG antibody NHS-ester activated gold nanoparticles. This protocol can also be adapted to any other primary amine containing biomolecule.

### Materials

- Antibody to be conjugated: 5–10 mg/mL in 1× Phosphate Buffered Saline (PBS), pH 7.4

**Note:** For effective conjugation, the purity of the protein must be considered. Any other molecules containing primary amines (e.g., TRIS) or other contaminating proteins (e.g., BSA) will compete with the protein to be conjugated and severely reduce the conjugation efficiency.

- 5–100 nm NHS-Activated Gold Nanoparticles (lyophilized from 2 mL, 1 OD) (See Product Table at the end of this section)
- Protein Resuspension/Reaction Buffer: 10–100 mM sodium phosphate, pH 7.8, 150 mM NaCl
- Quencher: 0.5 M Tris, pH 8.0
- Conjugate Storage Buffer: 20 mM Tris (pH 8.0), 150 mM NaCl, 1% BSA (w/v)

### Conjugation Protocol

1. Allow all reagents to warm to room temperature before use.
2. Dilute or dissolve the antibody in protein resuspension buffer to the final concentration indicated in **Table 3**.
3. In a microcentrifuge tube, combine the diluted protein sample with reaction buffer according to the table below.

	Conjugation Reaction (per vial of lyophilized NHS-gold nanoparticles)
Reaction Buffer	60 $\mu$ L
Diluted Protein Solution	48 $\mu$ L
Total Volume	108 $\mu$ L

4. Transfer 90  $\mu$ L of the protein/reaction buffer mix prepared in step 3 to one vial containing lyophilized NHS-activated gold nanoparticles and immediately mix well by pipetting up and down.

**Note:** Do not resuspend the lyophilized NHS-activated gold nanoparticles in buffer prior to addition of protein. NHS rapidly hydrolyzes in aqueous solution and will result in loss of conjugation efficiency.

- Incubate the vial at room temperature for 1–2 hours.
- Add 10  $\mu\text{L}$  of quencher solution to the vial to stop the reaction.
- Using a microcentrifuge, centrifuge the vial for 30 minutes using the appropriate speed for the gold nanoparticle size you are using according to **Table 2**.
- Discard the supernatant containing unbound protein.
- Add 100  $\mu\text{L}$  of gold conjugate storage buffer to the vial to resuspend your conjugate.

**Note:** Use a standard biological buffer compatible with your particular protein. For an antibody gold conjugate a suitable buffer is 20 mM Tris, pH 8.0, 150 mM NaCl, 1% (w/v) BSA.

- Record the UV/Vis spectrum of the conjugate using a spectrophotometer, and adjust concentration to an optical density of 10 using gold conjugate storage buffer.
- Perform functional test of conjugate (e.g., dot-blot or Western Blot)
- Store the gold conjugate at 2–8  $^{\circ}\text{C}$  until further use.

### Example Method IV: Conjugation of Antibodies to Maleimide-activated Gold Nanoparticles

This example protocol describes the covalent coupling of a standard IgG antibody to maleimide-activated gold nanoparticles. This protocol can also be adapted to any other thiol containing biomolecule such as a thiol-modified aptamer or oligonucleotide.

#### Materials

- Antibody to be conjugated

**Notes:** Maleimides react with thiols and depending on the type of protein, prior reduction of disulfide bonds, or modification of the biomolecule to carry a thiol group might be necessary.

For optimal conjugation efficiency avoid any contaminant(s) in the antibody solution such as BSA or thiol containing compounds such as DTT.

- 5–100 nm Maleimide-Activated Gold Nanoparticles (lyophilized from 2 mL, 1 OD) (See Product Table at the end of this section)
- Protein Resuspension Buffer: 10–100 mM sodium phosphate, pH 7.2, 150 mM NaCl
- Reaction Buffer: 10–100 mM sodium phosphate, pH 7.2, 150 mM NaCl
- Quencher: 10 mM Glutathione
- Conjugate Storage Buffer: 20 mM Tris, pH 8.0, 150 mM NaCl, 1% BSA (w/v)

### Conjugation Protocol

- Allow all reagents to warm to room temperature before use.
- Dilute or dissolve the antibody in protein resuspension buffer to the final concentration indicated in **Table 3**.
- In a microcentrifuge tube combine the diluted protein sample with reaction buffer according to the table below.

Conjugation Reaction (per vial of lyophilized maleimide-gold nanoparticles)	
Reaction Buffer	60 $\mu\text{L}$
Diluted Protein Solution	48 $\mu\text{L}$
Total Volume	108 $\mu\text{L}$

- Transfer 90  $\mu\text{L}$  of the protein/reaction buffer mix prepared in step 3 to one vial containing lyophilized Maleimide-activated gold nanoparticles and immediately mix well by pipetting up and down.

**Note:** Do not resuspend the lyophilized maleimide-activated gold nanoparticles in buffer prior to addition of protein. Maleimide hydrolyzes in aqueous solution and will result in loss of conjugation efficiency.

- Incubate the vial at room temperature for 1–2 hours.
- Add 10  $\mu\text{L}$  of quencher to the vial to stop the reaction.
- Using a microcentrifuge, centrifuge the vial for 30 minutes using the appropriate speed for the gold nanoparticle size you are using according to **Table 2**.
- Discard the supernatant containing unbound protein.
- Add 100  $\mu\text{L}$  of gold conjugate storage buffer to the vial to resuspend the conjugate.

**Note:** Use a standard biological buffer compatible with your particular protein. For an antibody gold conjugate a suitable buffer is 20 mM Tris, pH 8.0, 150 mM NaCl, 1% (w/v) BSA.

- Record the UV/Vis spectrum of the conjugate using a spectrophotometer, and adjust concentration to an optical density of 10 using gold conjugate storage buffer.
- Perform functional test of conjugate (e.g., dot-blot or Western Blot)
- Store the gold conjugate at 2–8  $^{\circ}\text{C}$  until further use.

#### References

- Njoki, P.N.; Lim, I.S.; Mott, D.; Park, H.; Khan, B.; Mishra, S.; Sujakumar, R.; Luo, J.; Zhong, C. *J. Phys. Chem. C*. **2007**, *111*, 14664–14669.
- Gilam, A.; Conde, J.; Weissglas-Volkov, D.; Oliva, N.; Friedman, E.; Artzi, N.; Shomron, N. *Nat. Commun.* **2016**, *7*, doi:10.1038/ncomms12868.
- Meir, R.; Shamalov, K.; Betzer, O.; Motiei, M.; Horovitz-Fried, M.; Yehuda, R.; Popovtzer, A.; Povotzer, R.; Cohen, C.J. *ACS Nano* **2015**, *9* (6), 6363–6372.
- O'Farrell, B. *The Immunoassay Handbook*. **2013**, *4*, 89–107.
- Fischer, N.O.; McIntosh, C.M.; Simard, J.M.; Rotello, V.M. *PNAS*, **2002**, *99* (8), 5018–5023
- Ni, Y.; Li, J.; Huang, Z.; He, K.; Zhuang, J.; Yang, W. *J. Nanopart. Res.* **2013** *15*:2038. doi:10.1007/s11051-013-2038-y
- Oliver, C. *Methods Mol. Biol.* **2010**, *588*, 369–373.

**Table 1.** Suggested Conjugation Optimization Grid (96 well plate) – Example Method I

Protein Added ( $\mu\text{g}$ )	pH Value												
	5.7	6.2	6.5	7.0	7.4	7.8	8.2	8.7	9.0	9.2	9.4	9.8	
0													
0.3													
0.6													
0.9													
1.2													
2													
4													
8													

**Table 2.** Centrifugation conditions for gold nanoparticles of various sizes.

Gold Nanoparticle Diameter	Centrifugation Force
10 nm	24,000 $\times g$ , 45 minutes
15 nm	15,000 $\times g$ , 30 minutes
20 nm	10,000 $\times g$ , 30 minutes
30 nm	2,500 $\times g$ , 30 minutes
40 nm	1,400 $\times g$ , 30 minutes
50 nm	1,100 $\times g$ , 30 minutes
60 nm	900 $\times g$ , 30 minutes
70 nm	700 $\times g$ , 30 minutes
80 nm	600 $\times g$ , 30 minutes
90 nm	500 $\times g$ , 30 minutes
100 nm	400 $\times g$ , 30 minutes

**Table 3.** Suggested IgG concentrations to be used for step 2 in the conjugation protocol based on the gold nanoparticle size to be conjugated. Note the concentrations in the table below are optimized for an antibody with a molecular mass of 150 kDa. For proteins differing significantly in molecular mass, the amount added to the reaction should be adjusted to represent the same molar amount and titrations may be necessary to determine the optimal concentration.

Gold Nanoparticle Diameter	Suggested Protein Concentration
5 nm	5 mg/mL
10 nm	3 mg/mL
15 nm	2 mg/mL
20 nm	1 mg/mL
30 nm	1 mg/mL
40 nm	0.5 mg/mL
50 nm	0.5 mg/mL
60 nm	0.5 mg/mL
70 nm	0.5 mg/mL
80 nm	0.5 mg/mL
90 nm	0.5 mg/mL
100 nm	0.5 mg/mL



# METHOD: Conjugating Gold Nanorods to Streptavidin and IgG



Christian Schoen

Nanopartz  
146 Barberrry Pl, Loveland, CO 80537  
cschoen@nanopartz.com  
Email: cschoen@nanopartz.com

## Introduction

The excellent optical properties of gold nanoparticles make them suitable for a broad range of applications extending from diagnostics to drug delivery and DNA therapy. However, in most cases, spherical gold nanoparticles exhibit absorption peaks at ~580 nm, well below the transmission window (650–900 nm) of most biological entities such as skin, tissue and hemoglobin. This limited wavelength window restricts the applications of spherical gold nanoparticles.

Gold nanorods exhibit many similar characteristics as gold nanoparticles, but they are elongated to optimize absorption and scattering properties. This ability to elongate the nanoparticle asymmetrically allows for tuning of the absorption between 550 nm to 1,400 nm, making gold nanorods attractive for applications in diagnostics. This protocol summarizes the conjugation and purification of non-surface functionalized gold nanorods to carboxyl groups and of carboxyl-functionalized nanorods to Streptavidin or IgG. The conjugation of carboxyl gold nanorods to Streptavidin or IgG essentially involves conjugation to an amine using EDC (1-ethyl-3-[3-dimethylaminopropyl] carbodiimide hydrochloride) (**Prod. No. E1769**), chemistry. This conjugation is important in biological applications including lateral flow diagnostics. Streptavidin and IgG are extensively used for tagging antigens and biotin.

EDC is a carboxyl and amine-reactive zero-length crosslinker. EDC reacts with a carboxyl group first and forms an amine reactive *O*-acylisourea intermediate that quickly reacts with an amino group to form an amide bond and release of an

isourea byproduct (see **Figure 1**). The intermediate is unstable in aqueous solutions, and therefore, two-step conjugation procedures require *N*-hydroxysuccinimide (**Prod. No. 130672**) for stabilization.<sup>1,2</sup> Failure to react with an amine results in hydrolysis of the intermediate, regeneration of the carboxyl, and release of an *N*-substituted urea. A side reaction is the formation of a *N*-acylurea, which is usually restricted to carboxyls located in hydrophobic regions of proteins.<sup>1,3</sup> EDC can be used to conjugate carboxyl to amine groups in peptides, proteins, and DNA labeling through 5' phosphate groups.

## Materials

1. Carboxyl-conjugated gold nanorods, 1.75 mg/mL, OD=50, 1 mL or gold nanorods (**Prod. Nos. 716812, 716820, 716839, 776688**) or CTAB-capped gold nanorods (**Prod. Nos. 900362, 900363, 900364, 900365, 900366, 900367**)
2. (±)- $\alpha$ -Lipoic acid (**Prod. No. T5625**)
3. *N*-(3-Dimethylaminopropyl)-*N'*-ethylcarbodiimide hydrochloride, 5 mg (**Prod. No. E1769**)
4. PBS Buffer, pH 7.4, 10 mL (**Prod. No. P4417**)
5. Streptavidin or IgG, 100  $\mu$ L, 1 mg/mL solution (**Prod. No. 85878**, Streptavidin, or specific IgG)
6. Ultra pure water, 10 mL
7. Low binding 2 mL microcentrifuge tube

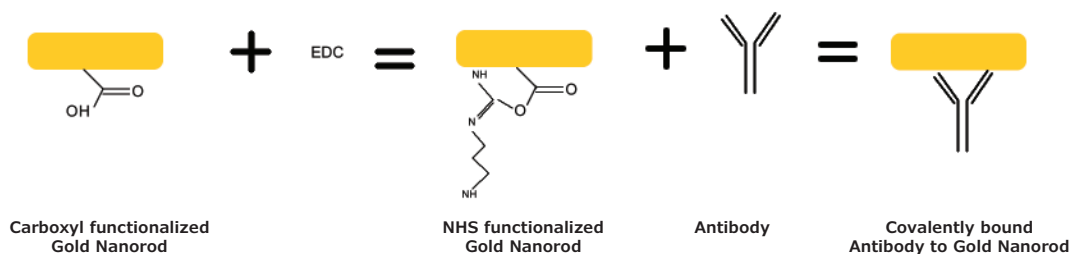


**Figure 1.** One-step EDC reaction with carboxyl and amine-containing molecules. EDC reacts with a carboxyl group first and forms an amine-reactive *O*-acylisourea intermediate that quickly reacts with an amino group to form an amide bond and release of an isourea byproduct.

### Storage and Shelf Life

Refrigerate at 4 °C. Shelf life is 14 days. Allow the components to warm to room temperature prior to using.

### Other Required Materials/Instruments

1. Transfer pipettes for volumes ranging from 1 µL to 2 mL
2. Microcentrifuge with minimum rcf = 10,000 for 20 nm sizes and larger; for smaller sizes, further optimization is required
3. Vortex for microcentrifuge tubes
4. Sonicator

### Other Optional Materials/Instruments

1. Dynamic light scattering (DLS)
2. Ultraviolet-visible spectrometer (UV/Vis)

### Procedure

This procedure details the process to make 5 OD-mls (optical density per milliliter) of conjugation of carboxyl-terminated gold. The first section details the functionalization steps of gold nanorods (**Prod. Nos. 716812, 716820, 716839, 776688**) to carboxyls.

1. Fill microcentrifuge tube with 2 mL of gold nanorods.
2. Add 25 µL of 1 mg/mL Lipoic Acid in water and vortex for 5 minutes.
3. Centrifuge the mixture for 5 minutes. The recommended centrifuge speed for **Prod. Nos. 716812** and **716820** is 12,000 rpm. For other nanorod products suggested centrifuge speed is 10,000 rpm for 5 minutes.

4. Remove supernatant and replace with MES (4-Morpholineethanesulfonic acid, **Prod. No. M3671**). Repeat this step twice.

The above steps should yield carboxyl functionalized gold nanorods ready for EDC chemistry. The carboxyl-functionalized gold nanorod is also available through MilliporeSigma (**Prod. No. 716898**).

The steps below illustrate the covalent binding of carboxyl-functionalized nanorods from above to streptavidin or IgG.

1. Fill microcentrifuge tube with 1.5 mL of water and add 40 µL of carboxyl-functionalized gold nanorods (**Prod. No. 716898**). Vortex for 5 seconds and save this as the control solution.
2. Add 100 µL of the rod solution to the 100 µL of IgG or Streptavidin.
3. Add 1 mL of ultra pure water.
4. Vortex for ~1 minute.
5. Add 1 mL water to 1 mg EDC and immediately add 100 µL of this stock solution to the stirred solution from step 4.
6. Vortex for 1 hour.
7. Spin in microcentrifuge at 13,000 rpm for 30 minutes or until a nice pellet is formed. Remove supernatant to less than 50 µL. Refill to 1.5 mL with phosphate-buffered saline (PBS). Repeat two more times. Sonicate between spins if necessary.
8. To ensure conjugation, measure the size and charge for both control and the product from step 7 using DLS. Note size increase and charge change by measuring a red shift on the UV/Vis, or overall increase in size using DLS sizing and DLS zeta.

### References

- (1) Grabarek, Z.; Gergely, J. *Anal. Biochem.* **1990**, *185*, 131–5.
- (2) Staros, J.V., et al. *Anal. Biochem.* **1986**, *156*, 220–2.
- (3) Timkovich, R. *Anal. Biochem.* **1977**, *79*, 135–43.

# METHOD: Directional Antibody Conjugation of Silica-coated Gold Nanoparticles



Justin Harris, Brantley Henson, Jason Cook, and Kimberly Homan\*

NanoHybrids Inc.  
3913 Todd Ln #310, Austin, TX 78744, USA  
\*Email: kimberly.homan@nanohybrids.net

## Introduction

Silica-coated gold nanoparticles (AuNP@SiO<sub>2</sub>) are plasmonic particles that can enhance imaging contrast in a variety of *in vitro* and *in vivo* optical imaging modalities. In particular, AuNP@SiO<sub>2</sub> are ideal for photoacoustic imaging. Key advantages of silica-coated gold nanoparticles include photoacoustic signal amplification and increased thermal stability over extended or repeated imaging sessions.<sup>1,2</sup> As many biological applications require molecular targeting, the method provided herein is intended to describe the directional bioconjugation of AuNP@SiO<sub>2</sub> to antibodies. The protocol can also be applied for conjugation of cysteine-rich proteins or other moieties featuring a free thiol group.

AuNP@SiO<sub>2</sub> are manufactured using a modified Stöber method.<sup>3,4</sup> This process utilizes the hydrolysis of tetraethyl orthosilicate (TEOS) to produce a silica coating on the gold surface. The resulting silica coating can be described accurately as a siloxane with terminal hydroxyl groups. Further adaptation of the modified Stöber method permits additional functionalization. For instance, functional groups can be added to the existing silica coating by the condensation of molecules containing both triethoxy-silane groups and a functional handle, such as maleimide (Figure 1). Biocompatibility and stability can be further enhanced through the use of methoxypolyethylene glycol-silane (mPEG-Sil) with a heterobifunctional PEG of choice.

Maleimide functionalized silica-coated particles are used to mediate directional antibody conjugation. Antibodies have a basic “Y” structure composed of two regions: the single-chain fragment crystallizable (F<sub>c</sub>) region and the fragment antigen-binding (F<sub>ab</sub>) region. As the name suggests, the F<sub>ab</sub> region (arms of the Y) is responsible for recognizing and binding to the desired antigen. Typical antibody conjugation techniques have no directionality, yielding nanoparticles with randomly oriented antibodies on their surface, decreasing overall antibody functionality. Additionally, directional antibody conjugation can reduce the amount of antibody required for effective targeting by covalently attaching the F<sub>c</sub> chain directly to the nanoparticle surface and ensuring the availability of F<sub>ab</sub> chains for antigen recognition.<sup>5</sup>

Maleimide-functionalized AuNP@SiO<sub>2</sub> are designed to mediate directional antibody conjugation through a thiol-hydrazide linker (HS-PEG-hydrazide) (Figure 2A). In preparation for conjugation, glycosyl groups found only on the non-targeting (F<sub>c</sub>) portion of the antibody are oxidized with sodium periodate to form aldehydes. The newly formed aldehydes readily react with hydrazide found on a HS-PEG-hydrazide linker to yield antibodies with a thiol-functionalized F<sub>c</sub> region. The terminal thiol groups can then spontaneously react with maleimide-functionalized AuNP@SiO<sub>2</sub> (Figure 2B).

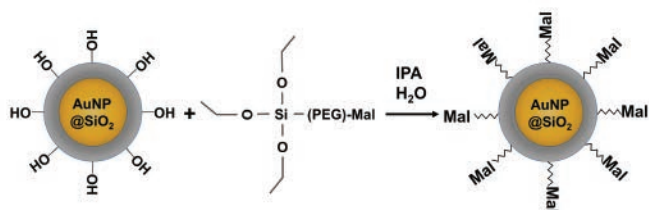
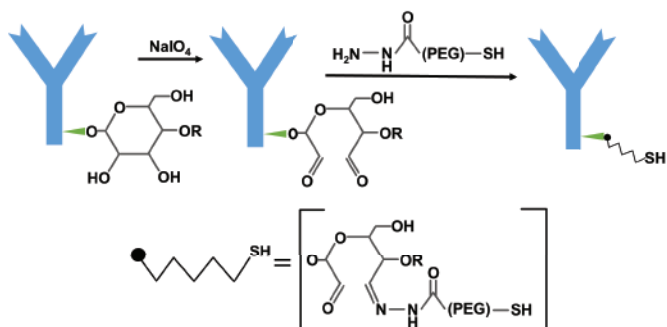
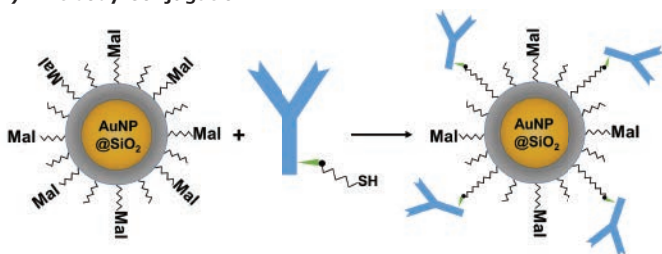


Figure 1. Maleimide (Mal) Functionalized Silica-coated Gold Nanoparticle

### A) Antibody Functionalization



### B) Antibody Conjugation



### C) Maleimide Passivation of Antibody Conjugated Particle

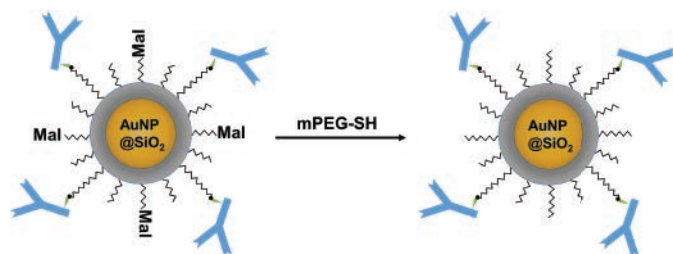


**Figure 2.** Directional Conjugation of Silica-coated Gold Nanoparticles

While this two-step functionalization method is robust, unreacted maleimide groups can remain on the  $\text{AuNP}@\text{SiO}_2$  surface. These unreacted maleimide groups are passivated through the addition of mPEG-SH, completing the conjugation (Figure 2C). This directional conjugation technique is only applicable for glycosylated antibodies, but this covers the majority of commercially-available IgG antibodies. The following example protocol describes directional antibody conjugation for maleimide-functionalized  $\text{AuNP}@\text{SiO}_2$ .

## Directional Antibody Conjugation

The following protocol can be used for the directional conjugation of glycosylated antibodies on the surface of maleimide-functionalized, silica-coated gold nanoparticles. This protocol is applicable for 10 nm diameter gold nanorods [750–900 nm surface plasmon resonance (SPR)] and 20 nm diameter gold nanospheres, each with 20 nm thick silica coatings. The

protocol can be adapted to other nanoparticle sizes by adjusting initial concentrations for nanoparticle surface area and is scalable. Nanoparticle concentration is given in terms of optical density (OD), defined as the absorbance of light as measured by a spectrophotometer through a 1 cm path length cuvette. The linked antibody can be prepared ahead of time and stored for the typical life of the antibody.

## Materials

- Sodium phosphate (chlorine-free) buffer, pH 7.5
- $\text{NaIO}_4$  (Prod. No. **769517**)
- PBS (Prod. No. **P5493**)
- 4-amino-3-hydrazino-5-mercapto-1,2,4-triazole (AHMT) solution
- SH-PEG-Hydrazide
- HEPES (Prod. No. **H4034**)
- 10 kDa Millipore® centrifuge filter
- Maleimide-functionalized, silica-coated gold nanoparticles at OD=2
- linked antibody solution
- 10 mg/mL mPEG-SH (5 kDa)
- 0.45  $\mu\text{m}$  pore size PVDF filter

## Part One: Preparation of the Linked Antibody

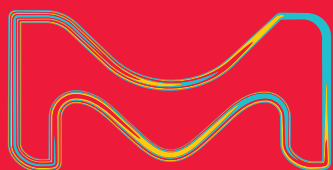
1. Freshly prepare 20  $\mu\text{L}$  of 1 mg/mL antibody solution in 100 mM sodium phosphate (chlorine-free) buffer, pH 7.5.
2. Prepare a fresh 100 mM solution of  $\text{NaIO}_4$  in water. Add 2  $\mu\text{L}$  of this solution to the antibody solution from step 1. Incubate in the dark for 30 minutes at room temperature (RT). This oxidizes the glycosylated region of the antibody to form aldehydes for coupling.
3. Quench the reaction with 100  $\mu\text{L}$  of 1 $\times$  PBS.
4. To verify oxidation of the carbohydrates, mix 5  $\mu\text{L}$  of the antibody solution with 15  $\mu\text{L}$  of freshly prepared 4-amino-3-hydrazino-5-mercapto-1,2,4-triazole (AHMT) solution (10 mg/mL AHMT dissolved in 1 M NaOH). The antibody-AHMT solution should turn purple in a few minutes to indicate the presence of aldehydes. If the solution remains clear or slightly yellow, then the antibody does not have a glycosylated region and this directional antibody conjugation method will not work. In this case, we suggest a non-directional conjugation scheme, as described previously in the literature.<sup>6</sup>
5. Add 2  $\mu\text{L}$  of 50 mM SH-PEG-Hydrazide in ethanol linker solution and incubate for 1 hour at RT. The SH-PEG-Hydrazide linker solution can be prepared ahead of time and stored at  $-20\text{ }^\circ\text{C}$  or  $-80\text{ }^\circ\text{C}$ .
6. Add 1 mL of 40 mM HEPES and filter through a 10 kDa Millipore® centrifuge filter (4 mL) at 4  $^\circ\text{C}$  and 2,000 rcf to purify. Resuspend in 200  $\mu\text{L}$  of 40 mM HEPES for a final concentration of 100  $\mu\text{g}/\text{mL}$ . At this point, the linked antibody can be stored at 4  $^\circ\text{C}$  for the recommended lifetime of the antibody.

## Part Two: Directional Antibody Conjugation with AuNP@SiO<sub>2</sub>

7. Prepare a solution of maleimide-functionalized, silica-coated gold nanoparticles at OD=2 in 40 mM HEPES at pH 8.5.
8. Add 200  $\mu\text{L}$  of linked antibody solution (20  $\mu\text{g}$ ) to 1 mL of nanoparticle solution. Incubate for 20 minutes at RT on a shaker table. If a higher degree of conjugation is desired, antibody mass can be increased up to 50  $\mu\text{g}$  (500  $\mu\text{L}$ ).
9. Add 100  $\mu\text{L}$  of freshly prepared 10 mg/mL mPEG-SH (5 kDa) in water to passivate any unreacted maleimide. Incubate for 20 minutes at RT on a shaker table.
10. Centrifuge at 4 °C and 10,000 rcf to pellet the antibody-conjugated nanoparticles. Remove the supernatant.
11. Resuspend in 1 mL of 1 $\times$  PBS or medium.
12. In sterile conditions, filter with a 0.45  $\mu\text{m}$  pore size PVDF filter.
13. A final yield of 60–80% from the initial AuNP@SiO<sub>2</sub> is expected. Little to no shift in the absorbance spectra should be observed upon successful conjugation and stabilization of the nanoparticles.
14. At this point, antibody-conjugated AuNP@SiO<sub>2</sub> can be stored at 4 °C for the recommended lifetime of the antibody. We recommend using an OD between 0.2 and 1 for *in vitro* cell-labeling experiments.

## References

- (1) Chen, Y.-S.; Frey, W.; Kim, S.; Kruizinga, P.; Homan, K.; Emelianov, S. *Nano Lett.* **2011**, *11*(2), 348–354.
- (2) Chen, Y.-S.; Frey, W.; Kim, S.; Homan, K.; Kruizinga, P.; Sokolov, K.; Emelianov, S. *Opt. Express* **2010**, *18*(9), 8867.
- (3) Stöber, W.; Fink, A.; Bohn, E. *J. Colloid Interface Sci.* **1968**, *26*(1), 62–69.
- (4) Lu, Y.; Yin, Y.; Mayers, B. T.; Xia, Y. *Nano Lett.* **2002**, *2*(3), 183–186.
- (5) Kumar, S.; Aaron, J.; Sokolov, K. *Nat. Protoc.* **2008**, *3*(2), 314–320.
- (6) Hermanson, G. T. *Bioconjugate Techniques (Third edition)*; Academic Press: Boston, **2013**.



# kits worth their weight

## Gold Nanoparticle and Nano-Urchin Conjugation Kits

Take advantage of the unique optical and biocompatible properties of gold nanoparticles and nanostructures without doing involved chemistry. Sigma-Aldrich Materials Science offers maleimide and *N*-hydroxysuccinimide (NHS) functionalized kits for one-step conjugation of oligonucleotides, antibodies, proteins, and peptides.

Gold nanoparticles can be used to target cells for imaging and photothermal therapy and drug delivery, detect biomarkers, conduct immunoassays, and more.

Kits come with lyophilized nanoparticles and ready to use mixtures. Easily screen antibodies or develop new diagnostics. No prior experience with conjugation is required.

Learn more at: [SigmaAldrich.com/biogold](http://SigmaAldrich.com/biogold)

Functional group	Particle size (nm)	Form	Peak SPR Wavelength (nm)	Product number
Maleimide	5	nanoparticle	515-520	<b>900458</b>
	20	nanoparticle	524	<b>900461</b>
	50	nano-urchin	585	<b>900484</b>
	70	nanoparticle	548	<b>900466</b>
	90	nano-urchin	630	<b>900488</b>
	100	nanoparticle	572	<b>900469</b>

Functional group	Particle size (nm)	Form	Peak SPR Wavelength (nm)	Product number
<i>N</i> -Hydroxy-succinimide	10	nanoparticle	515-520	<b>900473</b>
	30	nanoparticle	526	<b>900476</b>
	60	nano-urchin	585	<b>900491</b>
	80	nanoparticle	553	<b>900481</b>
	100	nano-urchin	680	<b>900493</b>

# Method: Covalent Bioconjugation of Antibodies to Carboxyl Terminated Nanoparticles



Rhea Decker, Steven J. Oldenburg\*

nanoComposix, Inc  
4878 Ronson Ct, San Diego, CA 92111  
\*Email: steve.oldenburg@nanocomposix.com

## Introduction

Conjugation of antibodies is commonly used as a means of targeting nanoparticles, either for diagnostics or for delivery of nanoparticles to a particular location *in vitro* or *in vivo*. In this article, we describe a method for covalently binding antibodies through an amide bond to the nanoparticle surface. There are many different methods for binding antibodies to a nanoparticle surface. For example, physisorption is a commonly used technique for gold nanoparticles because a clean surface on the gold nanoparticle exhibits a high affinity for the various functional groups present in an antibody. Such binding has been used for decades for the preparation of lateral flow diagnostics. However, the physisorption method has several drawbacks. These include: the release of the antibodies off the particles over time, difficulty in controlling the amount of antibody on the particles, and the need to optimize the exact conditions for the physisorption with each different antibody.

It has been found that the covalent bonding of antibodies through an amide bond from a free amine on the antibody to a carboxylic acid on the surface of nanoparticles is a simple and reproducible method for creating conjugates and for controlling the amount of antibody on the surface. In addition, in the case of conjugates used in lateral flow diagnostics, substantially less antibody is required to generate a functional conjugate. The example method we provide here has been optimized for 40 nm carboxyl functionalized (also known as lipoic acid functionalized) gold nanoparticles. Normalization for the total nanoparticle surface area in solution allows for extension of this chemistry to other sizes of nanoparticles with a carboxyl surface. In addition, by modifying the centrifugation parameters, the isolation of a variety of different particles can be achieved. For example, we have employed a similar method for carboxyl surfaced materials including gold nanoshells, gold rods, hollow gold spheres, spherical silver nanoparticles (lipoic acid functionalized), silver cubes, silica, quantum dots, and latex beads.

## Antibody Purification

Prior to conjugation, it is critical that the antibody solution does not contain additional free amines in the storage buffer as it will compete with binding sites on the nanoparticle. Free amines, including those found in tris buffer or the preservative sodium azide, must be removed and the antibody must be transferred to a suitable amine-free buffer. Likewise, any additional stabilizing proteins in the antibody solution must also be removed. Protein A or other affinity columns can be employed to isolate the antibody from other proteins. It is to be noted that the elution of the antibody from affinity columns often involves the use of amine containing buffers. A subsequent purification of the antibody into an amine-free buffer is then required. Steps involved in the purification of antibodies are detailed below.

## Materials

- Millipore Amicon Ultra 0.5 mL 10K filters for protein purification and concentration (**Prod. No. Z677108**)
- 2 mL Microcentrifuge tubes (to hold filters) (**Prod. No. Z628034**)
- Microcentrifuge
- Antibody to be purified
- Purification buffer (e.g., 10 mM potassium phosphate, or other amine-free buffer)
- Bicinchoninic acid (BCA) assay kit (**Prod. No. QPBCA**) and plate reader or UV/vis spectrophotometer for protein quantification

## Purification Protocol

1. Place filter inside microcentrifuge tube.
2. Add 450  $\mu$ L of purification buffer and centrifuge 5 minutes at 13,800 RCF to pre-rinse the filter.
3. Dispose of the filtrate at the bottom of the tube.
4. Aliquot antibody solution into filter and close cap.

**Note:** The filter can hold up to 500  $\mu\text{L}$ . If the volume to purify exceeds this capacity, centrifuge to concentrate and add more unpurified antibody before continuing with the wash steps. If the starting antibody volume is minimal, add buffer up to  $\sim 450 \mu\text{L}$  total volume.

5. Centrifuge 5 minutes at 13,800 RCF to concentrate.
6. Remove the filter containing the concentrated antibody from the microcentrifuge tube. Remove the filtrate solution from the bottom of the microcentrifuge tube.

**Note:** The filtrate can be retained from all wash steps in a clean container. If yield is particularly low due to punctured filter, the antibody may be reclaimed from retained filtrate.

7. Place the filter containing the concentrated antibody back into the tube and add 350  $\mu\text{L}$  of purification buffer to the filter.
8. Centrifuge for 5 minutes at 13,800 RCF to wash/concentrate.
9. Repeat washing procedure (steps 5–7 above) an additional four times using 350  $\mu\text{L}$  of additional purification buffer for a total of five washes.
10. After the final wash, turn device upside down in a *new, clean* 2 mL microcentrifuge tube and cut off the cap. Centrifuge 5 minutes at 1,000 RCF to collect purified and concentrated antibody. For optimal recovery, perform the reverse spin immediately.
11. Bring to final volume required so that the antibody concentration is  $\geq 1 \text{ mg/mL}$  for storage. After purification, typical recommended storage process is to aliquot the purified antibodies  $\geq 1 \text{ mg/mL}$  at  $-20 \text{ }^\circ\text{C}$ . Also freeze/thaw cycles should be avoided. However, antibody stability varies. Refer to antibody supplier for proper storage and handling.

### Determining Final Protein Concentration

Use  $A_{280}$  method or BCA assay to confirm concentration of starting material and final purified material to determine yield.

### Maximizing Sample Recovery

Low sample recovery in concentrate may be due to adsorptive losses, over-concentration, or passage of sample through the membrane. To maximize sample recovery, ensure that the pipette tip does not puncture the membrane filter. Adsorptive losses depend upon solute concentration, hydrophobicity, nature, temperature, time of contact with the filter device surfaces, sample composition, and pH. To minimize losses, remove concentrated samples immediately after centrifugation. If the starting sample concentration is high, monitor the centrifugation process in order to avoid over-concentration of the sample. Over-concentration can lead to precipitation and potential sample loss. If the sample appears to be passing through the membrane, choose a lower nominal molecular weight limit (NMWL) Amicon Ultra-0.5 filter unit. After collecting concentrated/purified antibody, the inside of the filter can be rinsed a few times with a small volume of purification buffer to reclaim any of the antibody that may be on the filter membrane.

### Conjugation to Nanoparticles

Antibodies can be conjugated to the terminal carboxylic acid functional groups on the surface of the nanoparticle through carbodiimide crosslinker chemistry (EDC). EDC reacts with the

carboxylic acid groups to form an active-ester intermediate. The addition of Sulfo-NHS increases solubility and stability of the intermediate, which reacts with the amine group of the antibody to form a stable amide bond between the antibody and nanoparticle. The method below describes the steps for antibody conjugation of carboxyl functionalized nanoparticle using gold nanoparticles as an example.

### Materials

- 40 nm carboxyl gold nanoparticles
- Purified antibody with no additional free amines
- Reaction buffer (5 mM potassium phosphate, 0.5% 20,000 MW PEG, pH 7.4)
- EDC (Prod. No. **E1769**)
- Sulfo-NHS (Prod. No. **56485**)
- Quencher (50% (w/v) hydroxylamine)
- Conjugate diluent (0.1 $\times$  PBS, 0.5% BSA)
- Centrifuge
- Standard microcentrifuge tubes (with no specialized treatments or residual plasticizer)
- Vortex
- Rotator

### Conjugation Protocol

The provided conjugation strategy can be adapted to any carboxyl functionalized nanoparticles. The example provided is intended for 1 mL of OD 20 40 nm diameter carboxyl gold nanoparticles that will result in 1 mL of antibody-gold conjugate at OD 20. For larger or smaller volumes, scale proportionately.

**IMPORTANT:** Steps 1–6 should be completed immediately after solubilizing EDC/Sulfo-NHS to minimize hydrolysis of the Sulfo-NHS ester in water and enhance the efficacy of conjugation.

1. Prepare EDC and Sulfo-NHS at 10 mg/mL in water immediately before conjugation steps.

**HINT:** Ensure the reagents are at room temperature before opening vials. Weigh out approximately 1–10 mg EDC and Sulfo-NHS each in individual microcentrifuge tubes. Just prior to conjugation, dissolve in the appropriate volume of water to bring the concentration to 10 mg/mL.

**Example:** Mass of EDC = 2.38 mg, add 238  $\mu\text{L}$  of  $\text{H}_2\text{O}$

Mass of Sulfo-NHS = 6.14 mg, add 614  $\mu\text{L}$  of  $\text{H}_2\text{O}$

2. Add 200  $\mu\text{g}$  of EDC (20  $\mu\text{L}$  of freshly prepared EDC at 10 mg/mL in  $\text{H}_2\text{O}$ ) and 400  $\mu\text{g}$  of Sulfo-NHS (40  $\mu\text{L}$  of freshly prepared Sulfo-NHS at 10 mg/mL in  $\text{H}_2\text{O}$ ) to 1 mL of 40 nm carboxyl gold nanoparticles.
3. Vortex solution and incubate at room temperature for 30 minutes while rotating.
4. Centrifuge at 3,600 RCF for 10 minutes.
5. Carefully remove supernatant to remove any excess EDC/Sulfo-NHS and resuspend in 1 mL of Reaction buffer. Vortex and/or sonicate to fully resuspend particles.
6. Add antibody and vortex solution.



7. Incubate at room temperature for 2 hours while rotating. Note that shorter or longer incubation times may improve the efficacy of conjugation.
8. After incubation, add 10  $\mu\text{L}$  of Quencher to deactivate any remaining active NHS-esters. Vortex and incubate at room temperature for 10 minutes while rotating.
9. Centrifuge at 3,600 RCF for 10 minutes. Carefully remove supernatant and resuspend in 1 mL of Reaction buffer. Vortex and/or sonicate to fully resuspend conjugate.
10. Repeat centrifugation and resuspension to remove any excess antibody.
11. Centrifuge again at 3,600 RCF for 10 minutes, remove supernatant, and bring volume up to 1 mL with Conjugate diluent. Vortex and/or sonicate to fully resuspend conjugate.
12. Store conjugate at 4  $^{\circ}\text{C}$ . Do not freeze.

### Optimizing the Conjugate

It is important to note that the optimal conjugation procedures are antibody dependent and the optimization techniques will differ between antibodies. The conjugates should be stable in solution and have efficient and specific binding to the antigen. The following tips can improve the efficacy of the conjugate.

- The activation of the carboxylic acid group with EDC and Sulfo-NHS is most efficient at pH 5.
- The pH of the reaction of primary amines on the antibody with the activated carboxyl groups is most efficient at pH 7-7.5. Performing the reaction at a higher pH drastically reduces the half-life of the NHS-ester intermediate.
- The concentration of the antibody during conjugation and the incubation time between the antibody and the nanoparticles can be adjusted to determine optimal conditions.
- The conjugate diluent components can be adjusted to determine the optimal buffer molarity, pH, blocking agents, polymers, and surfactants.

### Characterization of Conjugates

The characterization of conjugates is critical to ensure that the efficient binding of antibody to the surface of the particle and that the conjugate is stable. UV/Vis spectroscopy is one tool that can be utilized to evaluate the stability by looking at the plasmon resonance absorption. A slight shift in resonance peak position of the nanoparticle before and after conjugation indicates the antibody has been successfully conjugated to the surface. If the conjugate is aggregated, the peak shifts and becomes broader (**Figure 1**). Dynamic light scattering is another tool that can be used to screen for small amounts of aggregation by measuring the hydrodynamic size and the polydispersity index. Lateral flow test strips are also an effective way of evaluating conjugate performance, while also being a common application for such conjugates. The lateral flow test strip can contain reagents that are specific for the antibody conjugated to the nanoparticle and provides a fast and simple method for determining whether an antibody was successfully conjugated and still retains function.

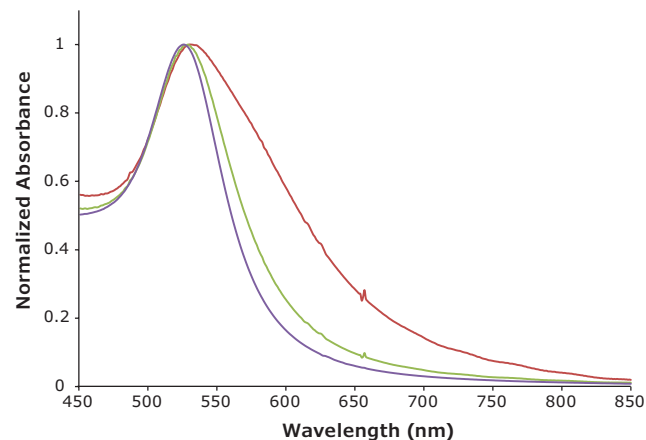


**Figure 1.** UV/Vis spectra of carboxyl terminated 40 nm Au (blue), protein conjugated gold (green) and aggregated 40 nm Au (red).

### References

- (1) Hermanson, G. T. *Bioconjugate Techniques (Third edition)*; Academic Press: Boston, 2013.

# Recommended Products for Diagnostics Using Optical Materials

## Gold Nanoparticles and Nanostructures

For more information on these materials, visit [SigmaAldrich.com/goldnanomaterials](http://SigmaAldrich.com/goldnanomaterials).

### Non-surface Functionalized Nanoparticles

Description	Particle Size (nm)	$\lambda_{max}$ (nm)	Concentration (particles/mL)	Prod. No.
reactant free stabilized suspension in 0.1 mM PBS	5	510-525	$\sim 5.5E+13$	752568-25ML 752568-100ML
	10	510-525	$\sim 6.0E+12$	752584-25ML 752584-100ML
	15	510-520	$\sim 1.64E+12$	777099-25ML 777099-100ML
	20	518-522	$\sim 6.54E+11$	753610-25ML 753610-100ML
	30	524-527	$\sim 1.8E+11$	753629-25ML 753629-100ML
	40	529-533	$\sim 7.2E+10$	753637-25ML 753637-100ML
	50	535-536	$\sim 3.5E+10$	753645-25ML 753645-100ML
	60	538-544	$\sim 1.9E+10$	753653-25ML 753653-100ML
	80	551-557	$\sim 7.8E+9$	753661-25ML 753661-100ML
	100	564-574	$\sim 3.8E+9$	753688-25ML 753688-100ML
	150	-	$\sim 3.6E+9$	746649-25ML 746649-100ML
	200	-	$\sim 1.9E+9$	746657-25ML 746657-100ML
	250	-	$\sim 7.1E+8$	746665-25ML 746665-100ML
	300	-	$\sim 4.5E+8$	746673-25ML
	400	-	$\sim 1.9E+8$	746681-25ML
	stabilized suspension in citrate buffer	5	510-525	$\sim 5.5E+13$
10		510-525	$\sim 6.0E+12$	741957-25ML 741957-100ML
15		510-525	$\sim 1.64E+12$	777137-25ML 777137-100ML
20		518-522	$\sim 7.2E+11$	741965-25ML 741965-100ML
30		524-527	$\sim 1.8E+11$	741973-25ML 741973-100ML
40		529-533	$\sim 7.2E+10$	741981-25ML 741981-100ML
50		535-539	$\sim 3.5E+10$	742007-25ML 742007-100ML
60		538-544	$\sim 1.9E+10$	742015-25ML 742015-100ML
80		551-557	$\sim 7.8E+9$	742023-25ML 742023-100ML
100		564-574	$\sim 3.8E+9$	742031-25ML 742031-100ML
150		-	$\sim 3.6E+9$	742058-25ML 742058-100ML
200		-	$\sim 1.9E+9$	742066-25ML 742066-100ML
250		-	$\sim 7.1E+8$	742074-25ML 742074-100ML
300		-	$\sim 4.5E+8$	742082-25ML
400		-	$\sim 1.9E+8$	742090-25ML
dispersion in H <sub>2</sub> O silica coated		5	-	$\sim 6.6E+13$
	10	514-524	$\sim 7.1E+12$	747564-5ML
	20	518-528	$\sim 8.5E+11$	747572-5ML

## Non-surface Functionalized Nanostructures

Name	Dimensions (nm)	$\lambda_{\max}$ (nm)	Concentration	Prod. No.
Gold microrods	diameter 200	-	50 $\mu\text{g}/\text{mL}$ in $\text{H}_2\text{O}$	716960-10ML
Gold nanorods	diameter 10	780	>30 $\mu\text{g}/\text{mL}$ in $\text{H}_2\text{O}$	716812-25ML
	diameter 10	780	>30 $\mu\text{g}/\text{mL}$ in $\text{H}_2\text{O}$	747971-5ML
	diameter 10	780	35 $\mu\text{g}/\text{mL}$ in $\text{H}_2\text{O}$	900362-25ML
	diameter 10	808	>30 $\mu\text{g}/\text{mL}$ in $\text{H}_2\text{O}$	716820-25ML
	diameter 10	808	>30 $\mu\text{g}/\text{mL}$ in $\text{H}_2\text{O}$	747998-5ML
	diameter 10	808	35 $\mu\text{g}/\text{mL}$ in $\text{H}_2\text{O}$	900363-25ML
	diameter 10	850	>30 $\mu\text{g}/\text{mL}$ in $\text{H}_2\text{O}$	716839-25ML
	diameter 10	850	>30 $\mu\text{g}/\text{mL}$ in $\text{H}_2\text{O}$	748005-5ML
	diameter 10	900	$\geq 30$ $\mu\text{g}/\text{mL}$ in $\text{H}_2\text{O}$	776653-25ML
	diameter 10	980	>30 $\mu\text{g}/\text{mL}$ in $\text{H}_2\text{O}$	776661-25ML
	diameter 10	980	>30 $\mu\text{g}/\text{mL}$ in $\text{H}_2\text{O}$	776688-25ML
	diameter 10	980	35 $\mu\text{g}/\text{mL}$ in $\text{H}_2\text{O}$	900364-25ML
	diameter 10	1064	35 $\mu\text{g}/\text{mL}$ in $\text{H}_2\text{O}$	900365-25ML
	diameter 25	550	>45 $\mu\text{g}/\text{mL}$ in $\text{H}_2\text{O}$	771643-25ML
	diameter 25	550	50 $\mu\text{g}/\text{mL}$ in $\text{H}_2\text{O}$	900366-25ML
	diameter 25	600	>45 $\mu\text{g}/\text{mL}$ in $\text{H}_2\text{O}$	771651-25ML
	diameter 25	650	>45 $\mu\text{g}/\text{mL}$ in $\text{H}_2\text{O}$	771686-25ML
	diameter 25	650	50 $\mu\text{g}/\text{mL}$ in $\text{H}_2\text{O}$	900367-25ML
diameter 25	-	100 $\mu\text{g}/\text{mL}$ in $\text{H}_2\text{O}$	716928-10ML	
diameter 25	-	100 $\mu\text{g}/\text{mL}$ in $\text{H}_2\text{O}$	716936-10ML	
Gold, nano-urchins	avg. part. size 50	585	0.1 mM in PBS	795380-25ML
	avg. part. size 60	585	0.1 mM in PBS	795399-25ML
	avg. part. size 90	630	0.1 mM in PBS	797707-25ML
	avg. part. size 80	620	0.1 mM in PBS	797723-25ML
	avg. part. size 70	600	0.1 mM in PBS	797731-25ML
	avg. part. size 100	680	0.1 mM in PBS	797758-25ML

## Surface-functionalized Nanoparticles and Nanostructures

Name	Description	Dimension (nm)	Absorption (nm)	Prod. No.
Gold nanoparticles	PEG 3000 coated amine functionalized	diameter 5	515	765260-1ML
		diameter 10	520	765295-1ML
		diameter 15	520	765317-1ML
		diameter 20	520	765333-1ML
		diameter 30	525	765368-1ML
		diameter 40	530	765384-1ML
	PEG 5000 coated amine functionalized	diameter 5	515	765279-1ML
		diameter 10	520	765309-1ML
		diameter 15	520	765325-1ML
		diameter 20	520	765341-1ML
		diameter 30	525	765376-1ML
		diameter 50	535	765414-1ML
	PEG 5000 biotin terminated	diameter 5	513-517	808628-0.5ML
		diameter 10	515-520	808709-0.5ML
		diameter 15	520	808830-0.5ML
		diameter 20	524	808849-0.5ML
		diameter 30	526	808857-0.5ML
		diameter 40	530	808865-0.5ML
		diameter 50	535	808903-0.5ML
		diameter 60	540	808911-0.5ML
		diameter 70	548	808938-0.5ML
		diameter 80	553	808946-0.5ML
		diameter 90	564	808954-0.5ML
		diameter 100	572	808962-0.5ML

Name	Description	Dimension (nm)	Absorption (nm)	Prod. No.
Gold nanoparticles	PEG 3000 coated carboxylic acid functionalized	diameter 5	515	765430-1ML
		diameter 10	520	765457-1ML
		diameter 15	520	765473-1ML
		diameter 20	520	765503-1ML
		diameter 30	525	765538-1ML
		diameter 40	530	765554-1ML
	PEG 5000 coated carboxylic acid functionalized	diameter 5	515	765449-1ML
		diameter 10	530	765465-1ML
		diameter 15	520	765481-1ML
		diameter 30	525	765546-1ML
		diameter 20	520	765511-1ML
		diameter 40	530	765562-1ML
	PEG 2000 coated methyl terminated	diameter 15	520	765694-1ML
		diameter 20	520	765716-1ML
	PEG 5000 coated methyl terminated	diameter 5	515	765600-1ML
		diameter 15	520	765708-1ML
		diameter 20	520	765724-1ML
		diameter 30	525	765732-1ML
Gold nanoparticles dodecanethiol functionalized	nanoparticles	diameter 50	535	765686-1ML
		particle size 3 - 5	-	660434-5ML
Gold nanoparticles octanethiol functionalized	nanoparticles	avg. part. size 2 - 4	-	660426-5ML
Gold nanorods	amine terminated	diameter 10	808	716871-1ML
	carboxyl terminated	diameter 10	808	716898-1ML
	methyl terminated	diameter 10	808	716901-1ML

## Surface-functionalized Nanoparticle and Nanostructure Kits

Name	Functional Group	Particle Size (nm)	$\lambda_{max}$ (nm)	Prod. No.
Gold nanoparticles	maleimide	5	515-520	900458-1EA
	maleimide	15	520	900460-1EA
	maleimide	20	524	900461-1EA
	maleimide	30	526	900462-1EA
	maleimide	40	530	900463-1EA
	maleimide	50	535	900464-1EA
	maleimide	60	540	900465-1EA
	maleimide	70	548	900466-1EA
	maleimide	80	553	900467-1EA
	maleimide	90	564	900468-1EA
	NHS	5	515-520	900470-1EA
	NHS	10	515-520	900473-1EA
	NHS	15	520	900474-1EA
	NHS	20	524	900475-1EA
	NHS	30	526	900476-1EA
	NHS	40	530	900477-1EA
	NHS	50	535	900478-1EA
	NHS	60	540	900479-1EA
	NHS	70	548	900480-1EA
	NHS	80	553	900481-1EA
Gold nano-urchins	maleimide	90	564	900482-1EA
	NHS	100	572	900483-1EA
	maleimide	50	585	900484-1EA
	maleimide	60	585	900485-1EA
	maleimide	70	600	900486-1EA
	maleimide	80	620	900487-1EA
	maleimide	90	630	900488-1EA
	maleimide	100	680	900489-1EA
	NHS	50	585	900490-1EA
	NHS	60	585	900491-1EA
	NHS	70	600	900492-1EA
	NHS	80	620	900493-1EA
	NHS	90	630	900494-1EA
	NHS	100	680	900495-1EA

## Silver Nanoparticles and Nanostructures

For more information on these materials, visit [SigmaAldrich.com/silvernanomaterials](https://www.sigmaaldrich.com/silvernanomaterials).

### Silver Nanoparticles

Functional Group	Concentration	Average Particle Size (nm)	$\lambda_{\text{max}}$ (nm)	Prod. No.
BPEI	0.02 mg/mL in water	10	400	796379-25ML
	0.02 mg/mL in water	20	400	796387-25ML
	0.02 mg/mL in water	30	415	796395-25ML
	0.02 mg/mL in water	40	415	796409-25ML
	0.02 mg/mL in water	50	425	796417-25ML
	0.02 mg/mL in water	60	435	796425-25ML
	0.02 mg/mL in water	80	470	796433-25ML
	0.02 mg/mL in water	100	495	796441-25ML
	0.02 mg/mL in water	200	500	796468-25ML
	1.10 mg/mL in water	60	496	809462-1ML
	1 mg/mL in water	40	420	807575-1ML
	1 mg/mL in water	50	420	807583-1ML
	1 mg/mL in water	80	460	807567-1ML
	1 mg/mL in water	100	490	807559-1ML
	1 mg/mL in water	200	515	807540-1ML
citrate	0.02 mg/mL (in 2 nM aqueous sodium citrate)	30	400	796123-25ML
	0.02 mg/mL (in 2 nM aqueous sodium citrate)	50	420	796131-25ML
	0.02 mg/mL (in 2 nM aqueous sodium citrate)	80	455	796158-25ML
	0.02 mg/mL (in 2 nM aqueous sodium citrate)	200	485	796166-25ML
	1 mg/mL (aqueous sodium citrate)	10	390	806978-1ML
	1 mg/mL (aqueous sodium citrate)	20	390	806986-1ML
	1 mg/mL (aqueous sodium citrate)	30	400	806994-1ML
	1 mg/mL (aqueous sodium citrate)	40	415	807001-1ML
	1 mg/mL (aqueous sodium citrate)	50	420	807028-1ML
	1 mg/mL (aqueous sodium citrate)	60	430	807036-1ML
	1 mg/mL (aqueous sodium citrate)	80	455	807044-1ML
	1 mg/mL (aqueous sodium citrate)	100	485	807141-1ML
	1 mg/mL (aqueous sodium citrate)	200	480	807133-1ML
lipoic acid	0.02 mg/mL in water	20	400	796182-25ML
	0.02 mg/mL in water	30	410	796190-25ML
	0.02 mg/mL in water	40	415	796204-25ML
	0.02 mg/mL in water	50	420	796212-25ML
	0.02 mg/mL in water	60	430	796220-25ML
	0.02 mg/mL in water	80	470	796239-25ML
	0.02 mg/mL in water	100	485	796247-25ML
	0.02 mg/mL in water	200	490	796255-25ML
	1 mg/mL in water	40	415	807249-1ML
	1 mg/mL in water	50	430	807257-1ML
	1 mg/mL in water	60	430	807370-1ML
	1 mg/mL in water	80	470	807362-1ML
	1 mg/mL in water	100	490	807354-1ML
	1 mg/mL in water	200	490	807346-1ML
	PEG	0.02 mg/mL in water	40	410
0.02 mg/mL in water		50	420	796328-25ML
0.02 mg/mL in water		60	430	796336-25ML
0.02 mg/mL in water		80	470	796344-25ML
0.02 mg/mL in water		100	485	796352-25ML
0.02 mg/mL in water		200	500	796360-25ML
1 mg/mL in water		40	410	807281-1ML
1 mg/mL in water		50	420	807400-1ML
1 mg/mL in water		60	430	807419-1ML
1 mg/mL in water		80	460	807427-1ML
1 mg/mL in water		100	490	807435-1ML
1 mg/mL in water		200	495	807443-1ML

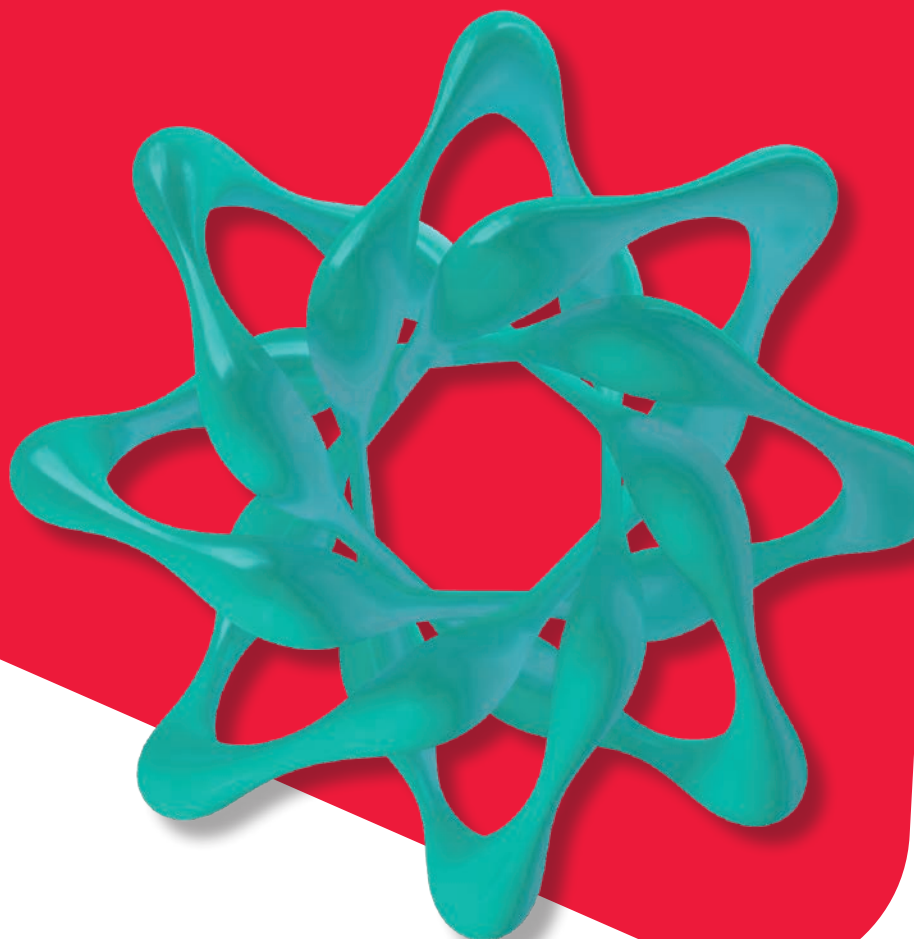
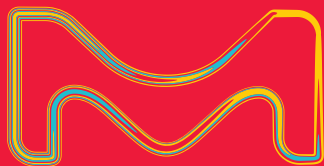
Functional Group	Concentration	Average Particle Size (nm)	$\lambda_{\text{max}}$ (nm)	Prod. No.
PVP	0.02 mg/mL in water	20	395	795933-25ML
	0.02 mg/mL in water	10	390	795925-25ML
	0.02 mg/mL in water	30	400	795941-25ML
	0.02 mg/mL in water	40	410	795968-25ML
	0.02 mg/mL in water	50	425	795976-25ML
	0.02 mg/mL in water	80	460	795992-25ML
	0.02 mg/mL in water	200	485	796026-25ML
	0.02 mg/mL in water	60	430	795984-25ML
	0.02 mg/mL in water	100	480	796018-25ML
	1 mg/mL in water	40	415	807095-1ML
	1 mg/mL in water	50	415	807087-1ML
	1 mg/mL in water	60	430	807079-1ML
	1 mg/mL in water	80	455	807184-1ML
	1 mg/mL in water	100	485	807192-1ML
	1 mg/mL in water	200	480	807206-1ML

## Silver Nanoplates

Functional Group	Concentration	$\lambda_{\text{abs}}$ (nm)	Prod. No.
PVP	0.02 mg/mL (in water with 5 mM sodium borate buffer)	550	796476-25ML
	0.02 mg/mL (in water with 5 mM sodium borate buffer)	650	796484-25ML
	0.02 mg/mL (in water with 5 mM sodium borate buffer)	750	796492-25ML
	0.02 mg/mL (in water with 5 mM sodium borate buffer)	850	796506-25ML
	0.02 mg/mL (in water with 5 mM sodium borate buffer)	950	796514-25ML
	0.02 mg/mL (in water with 5 mM sodium borate buffer)	1050	796522-25ML
	~1 mg/mL (in water with 5 mM sodium borate buffer)	550	807532-1ML
	~1 mg/mL (in water with 5 mM sodium borate buffer)	650	807524-1ML
	~1 mg/mL (in water with 5 mM sodium borate buffer)	750	807516-1ML
	~1 mg/mL (in water with 5 mM sodium borate buffer)	850	807699-1ML
	~1 mg/mL (in water with 5 mM sodium borate buffer)	950	807680-1ML
	~1 mg/mL (in water with 5 mM sodium borate buffer)	1050	807672-1ML

**Sigma-Aldrich®**

Lab Materials & Supplies



# Inking outside the BOX

Select. Formulate. Print.

Our new graphene ink formulation can be printed into 3D graphene structures that have potential applications in tissue engineering and regenerative medicine as well as in electronic devices.

## Graphene Ink for 3D Printing

- Moderate viscosity
- Use with 50-2,000  $\mu\text{m}$  nozzles
- Rapid solidification: No drying time is required after printing
- High graphene content  
60 vol% graphene and 40 vol% biocompatible elastomeric polymer in the resulting 3D printed material
- Excellent electrical conductivity  
As printed, greater than 650 S/m; after annealing at 50 °C, greater than 850 S/m
- Bioactive and potentially biocompatible

Particle Size ( $\mu\text{m}$ )	Viscosity (Pa.s)	Resistivity ( $\Omega/\text{cm}$ )	Product number
1-20 (length and width) 1-15 (thick)	25-45 (At low shear stresses. Shear thins to $\sim$ 10-15 Pa.s at Shear Stress = 100 Pa	0.12-0.15 (as 3D-printed fibers, not ink, 200-400 $\mu\text{m}$ diameter)	808156

[SigmaAldrich.com/conductive3d](http://SigmaAldrich.com/conductive3d)

The life science business of Merck operates as MilliporeSigma in the U.S. and Canada.

**MERCK**

[SigmaAldrich.com/nanomaterials-conjugation](http://SigmaAldrich.com/nanomaterials-conjugation)

